Elettra Sincrotrone Trieste

X-ray imaging and tomography for biomedical research

Giuliana Tromba

Elettra - Sincrotrone Trieste

SYnchrotron **R**adiation for **ME**dical **P**hysics (SYRMEP) beamline

School on Synchrotron and Free-Electron-Laser Based Methods:
Multidisciplinary Applications and Perspectives,
ICTP – Miramare, 4-15 April 2016

The Abdus Salam International Centre for Theoretical Physics

Elettra Sincrotrone Trieste

Outline

- Characteristics and potentials of synchrotron X-rays
- SR X-rays imaging techniques
  - Absorption, K-edge imaging
  - Phase contrast techniques:
    - *Propagation Based Imaging (PBI)*
    - *Analizer Based Imaging (ABI)*
    - *X-ray interferometry with crystals*
    - *Grating interferometric imaging (GI)*
    - *Grating non-interferometric imaging*
- Applications in the life sciences
  - Bronchography
  - Mammography
  - Studies of bones, joints and cartilages
  - Lungs imaging
  - Brain studies
  - Imaging of atherosclerotic plaques
- Quantitative analysis

Advantages of SR for biomedical imaging

Monochromaticity allows for:

- *optimization* of X-ray energy according to the specific case under study (dose reduction)
- quantitative CT evaluations
- no beam hardening
- convenient use of contrast agent (K-edge and L-edge imaging)

Spatial coherence enables the applications of ***phase sensitive imaging techniques***

- Phase contrast overcomes the limitation of conventional radiology
- It brings to a dose reduction
- Improved contrast resolution, edges enhancement
- Use of phase retrieval algorithms

High fluxes

- Short exposure time
- Dynamic studies….

Collimation

- parallel beams, scatter reduction
- beam shaping (micro-beams)

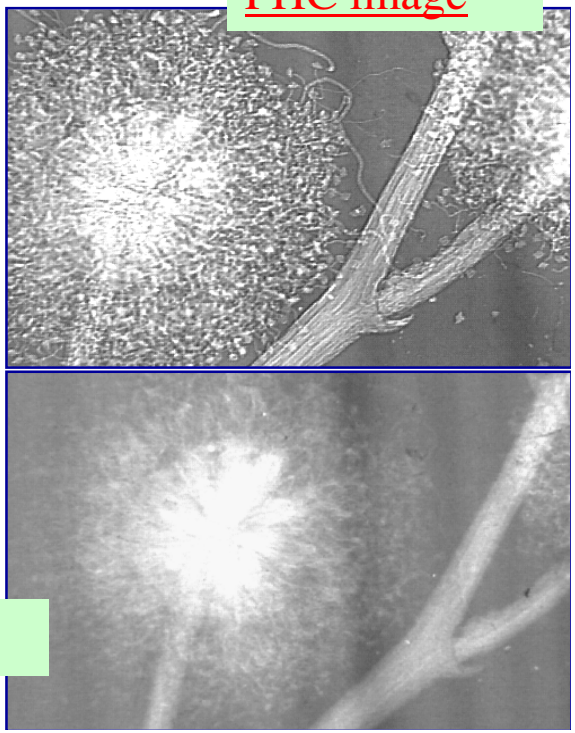

Different imaging approaches

- Clinical: applications to patients
  (es. mammography, angiography, ecc.)
  *Need to **limit** radiation dose. Find best compromise between dose and image quality*

- Imaging of small animals: applied for different purposes in the development of ***animal models***
  (es. Cell tracking, Osteoporosis, genetic diseases,..)
  Research protocols, control of dose.

- "In vitro" imaging: it concerns the study of biological samples. (es. micro-tomography applied on bone samples, scaffolds, cartilages, etc.)
  Requirements of high resolution and high sensitivity

Elettra Sincrotrone Trieste

SR X-rays imaging techniques

1) K-edge subtraction imaging

Exploiting the monochromaticity of SR…

K-edge Subtraction Imaging

1. Contrast agent: Iodine, or Gadolinium, etc.
2. Two Images are acquired : Above (A) and Below (B) the K-edge
3. Image processing : Iodine and Tissue images

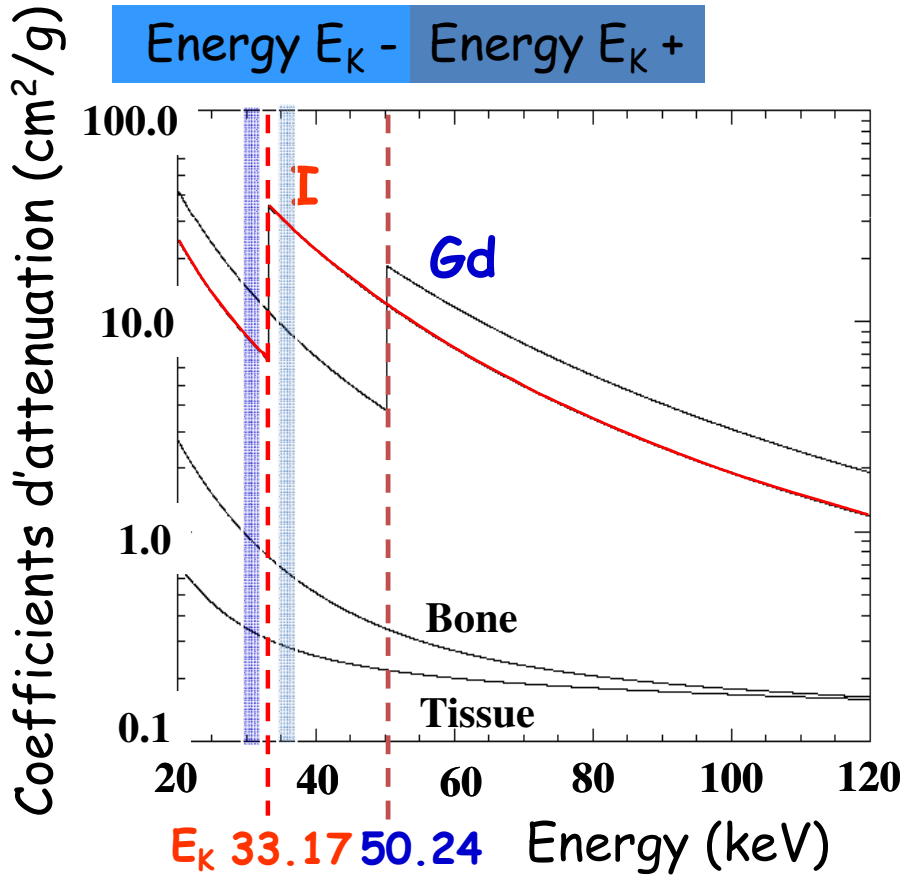

$$x_i = \frac{\mu_{Bi}\ln(A) - \mu_{Ai}\ln(B)}{\mu_{Bi}\mu_{At} - \mu_{Ai}\mu_{Bt}}$$

$$x_t = \frac{\mu_{Bi}\ln(A) - \mu_{Ai}\ln(B)}{\mu_{Bi}\mu_{At} + \mu_{Ai}\mu_{Bt}}$$

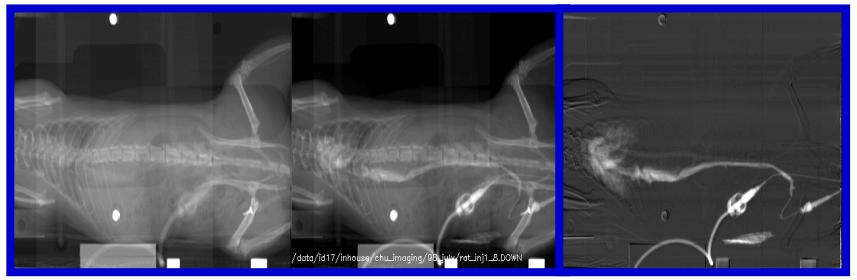

Below Above K-edge

Iodine Image

Courtesy of A.Bravin (ESRF)

Elettra Sincrotrone Trieste

2 - *Phase – contrast* imaging techniques: main cathegories

Propagation-based Imaging (PBI)

Analizer-Based Imaging (ABI)

X-ray interferometry with crystals

Grating interferometric imaging (GI)

Grating non-interferometric imaging

Exploiting the spatial coherence of SR…

Phase-sensitive imaging techniques

Conventional radiology relies on X-ray absorption as the unique source of contrast and is based exclusively on the detection of amplitude variation of the transmitted X-rays
Main limitation:poor contrast for samples with low-Z composition.

Phase sensitive imaging techniques are based on the observation of the *phase shifts* produced by the object on the incoming wave.

Refractive index: $n = 1 - \delta + i\beta$
β = absorption term; δ = phase shift term
$\beta \sim 10^{-10}$; $\delta \sim 10^{-6}$ in soft tissue @ 17 keV
$\delta \propto \lambda^2$, $\beta \propto \lambda^3$
Absorption radiology -> contrast generated by differences in the x-ray absorption ($\beta \Delta z$)
Phase Radiology –> contrast generated by phase shifts
$\delta >> \beta$ –> phase contrast >> absorption contrast

Conventional imaging vs. *Phase contrast*

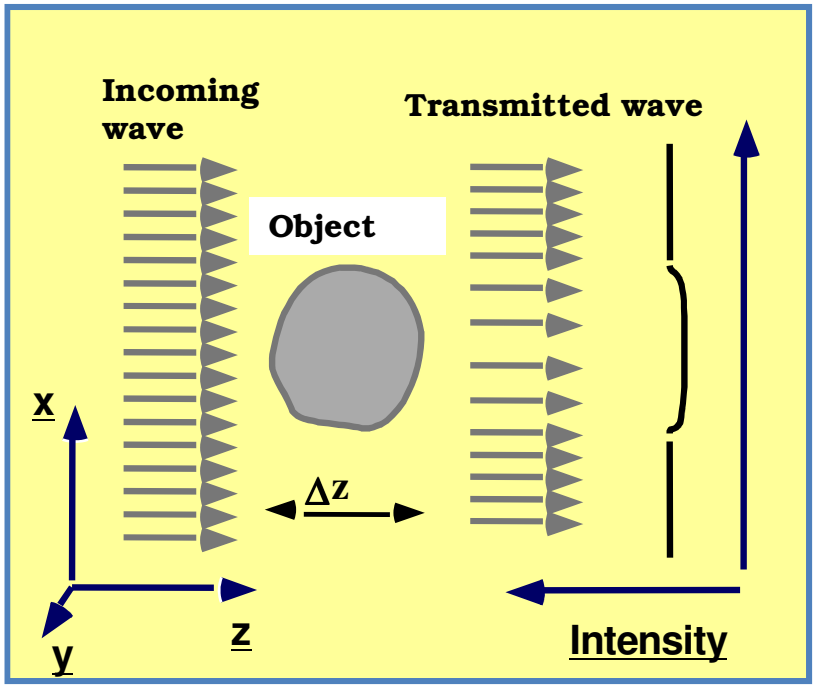

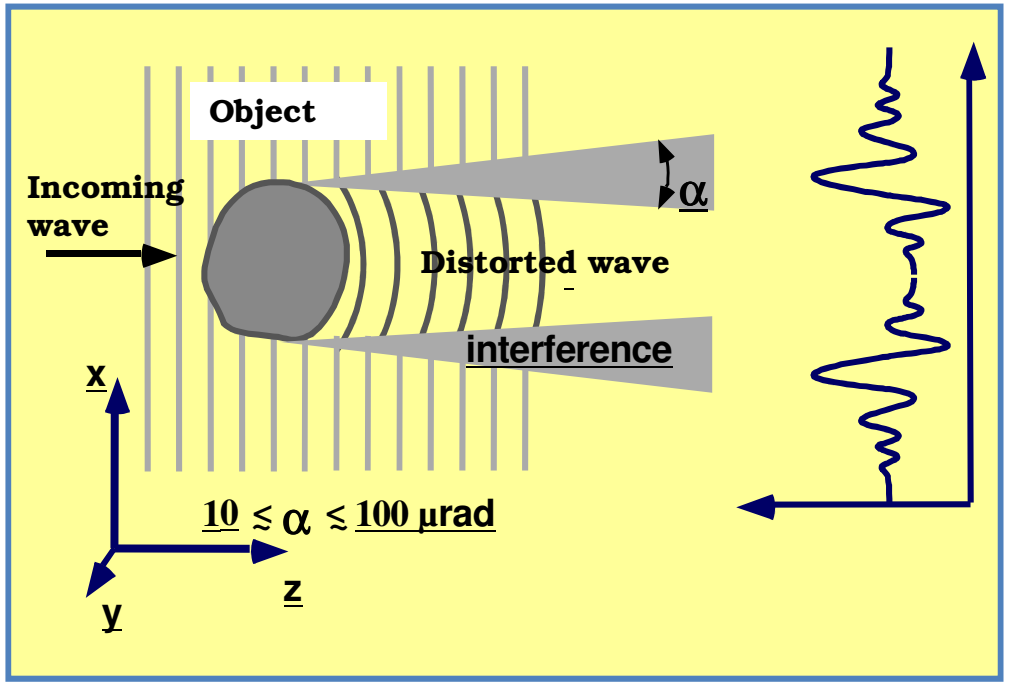

Conventional imaging (absorption)

Phase contrast

Propagation based imaging (PBI)

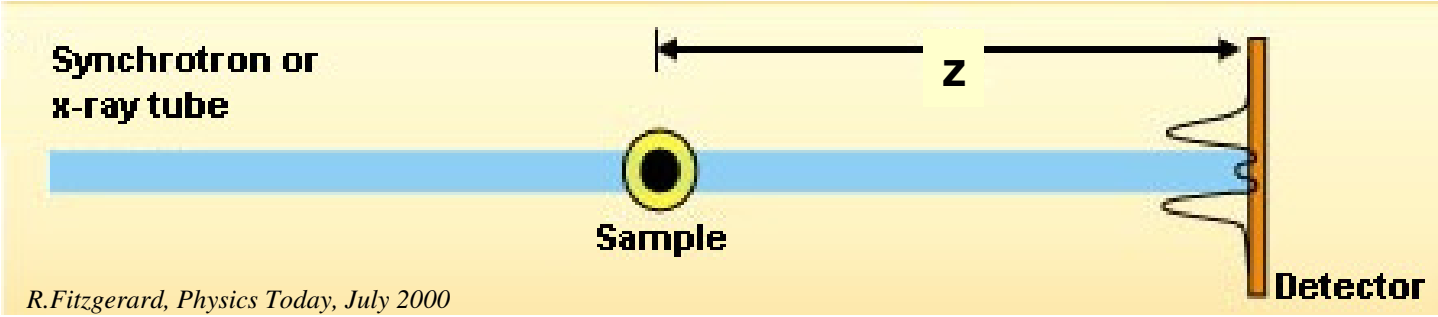

R.Fitzgerard, Physics Today, July 2000

- The technique exploits the high spatial coherence of the X-ray source.
- z =0 -> absorption image
- For z > 0 -> interference between diffracted and un-diffracted wave produces edge and contrast enhancement. A variation of δ is detected
- Measure of $\nabla^2\Phi(x,y)$
- The technique requires a high spatial coherence source, monochromaticity is not needed

Regimes

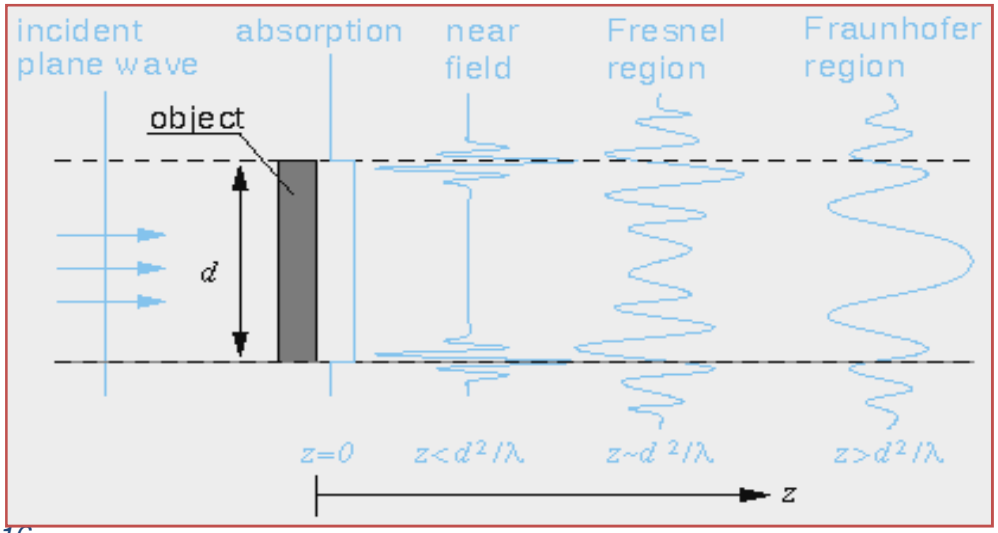

Snigirev A. et al., Rev. Sci. Instrum. 66, 1995
Wilkins S. W. et al., Nature 384, 1996
Cloetens P. et al., J. Phys D: Appl. Phys. 29, 1996
Arfelli F et al., Phys. Med. Biol. 43,1998

Analyzer Based Imaging (ABI)

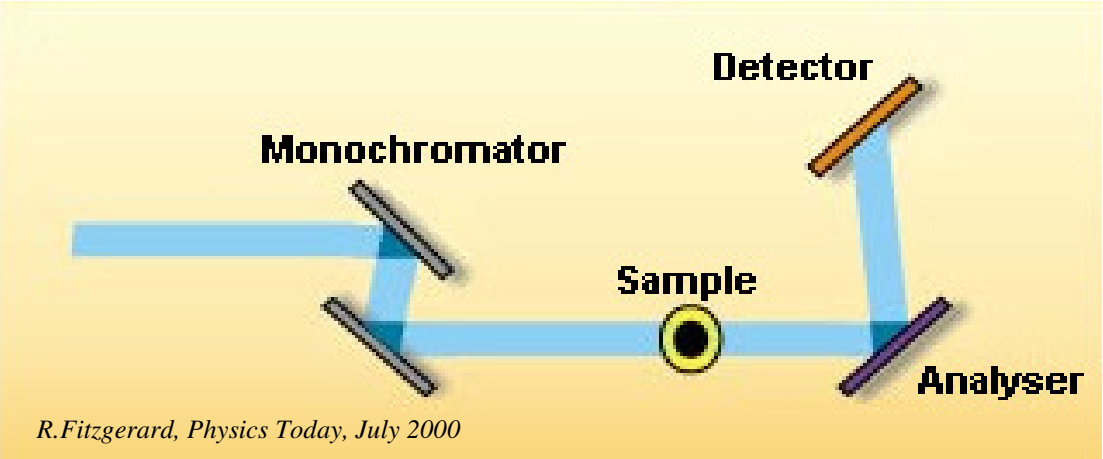

R.Fitzgerard, Physics Today, July 2000

- A perfect crystal is used as an angular filter to select angular emission of X-rays. The filtering function is the rocking curve (FWHM: 1-20 μrad)
- Image formation with ABI is sensitive to a variation of δ in the sample. Indeed, **refraction angle is roughly proportional to the gradient of δ**
- Analyzer and monochromator aligned -> X-ray scattered by more than some tens μrad are rejected
- Small misalignments -> investigation of phase shift effects
- With greater misalignments the primary beam is almost totally rejected and pure refraction images are obtained
- Sensitive to $\nabla\Phi(x,y)$
- The technique requires the beam monochromaticity.

Podurets K. M. et al., Sov. Phys. Tech. Phys. 34(6), 1989
V. N. Ingal and E. A. Beliaevskaya, J. Phys. D: Appl. Phys. 28, 1995
Chapman D et al., Phys. Med. Biol. 42, 1997

ABI image manipulation (original algorithm)

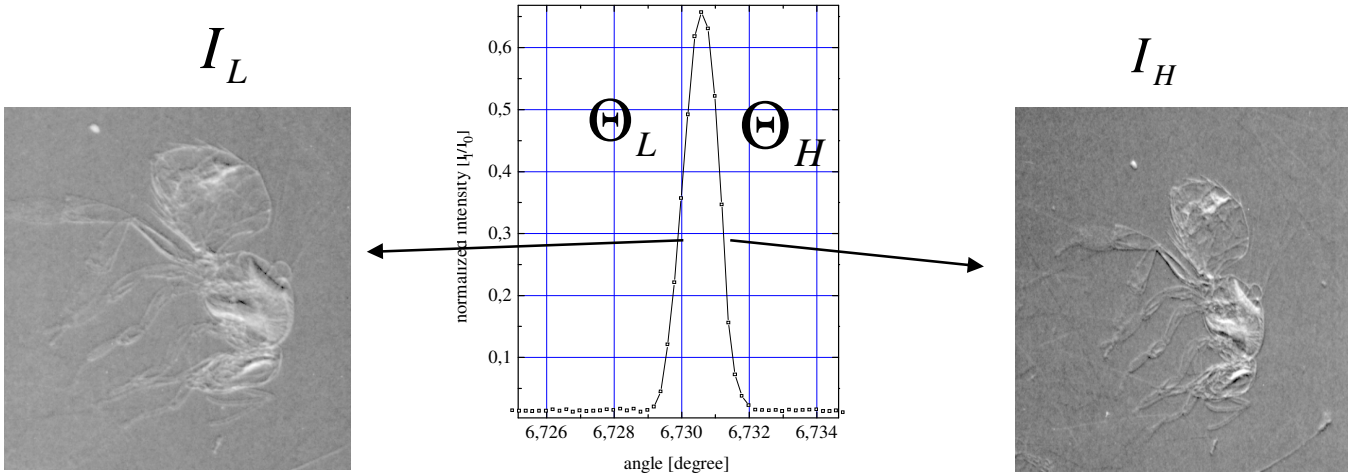

Linear approximation of rocking curve at half values (I_R and I_L)

$$I_L = I_R\left(R(\Theta_L) + \frac{\partial R}{\partial \Theta}(\Theta_L)\Delta\Theta_z \right)$$

$$I_H = I_R\left(R(\Theta_H) + \frac{\partial R}{\partial \Theta}(\Theta_H)\Delta\Theta_z \right)$$

Θ_Z = refraction Image

I_R = apparent absorption image
(absorption+extinction)

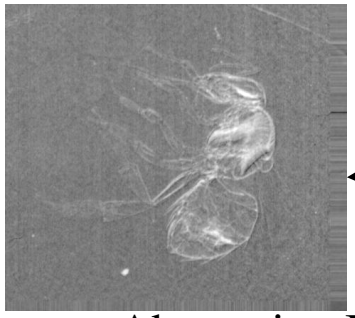

Apparent Absorption Image

$$I_R = \frac{I_L \cdot \left.\frac{dR}{d\Theta}\right|_{\Theta_H} - I_H \cdot \left.\frac{dR}{d\Theta}\right|_{\Theta_L}}{R(\Theta_L)\cdot \left.\frac{dR}{d\Theta}\right|_{\Theta_H} - R(\Theta_H)\cdot \left.\frac{dR}{d\Theta}\right|_{\Theta_L}}$$

$$\Theta_Z = \frac{I_H \cdot R(\Theta_L) - I_L \cdot R(\Theta_H)}{I_L \cdot \left.\frac{dR}{d\Theta}\right|_{\Theta_H} - I_H \cdot \left.\frac{dR}{d\Theta}\right|_{\Theta_L}}$$

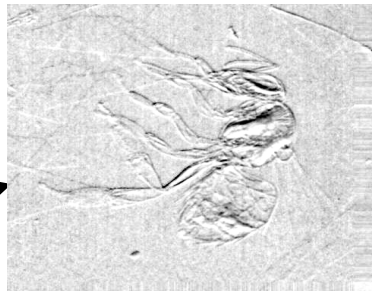

Refraction Image

Ref: Chapman et al, Phys.Med.Biol, 42,1997

Limitations and Requirements

PBI

- It is the simplest method as it requires the detector to be set at a certain distance from the sample. It does not require monochromaticity.
- Requirements:
  - a high spatial coherence of the beam
  - adequate spatial resolution of the detector to detect interference fringes (edge-enhancement)
- Exposure time related to beam intensity
- The recorded signal is proportional to the second derivative of the phase term ($\nabla^2\Phi(x,y)$)
- Adequate to study samples with important variations of refractive index

ABI

- It requires the implementation and control of at least one crystal
- Requirements:
  - high monochromaticity
  - parallel beam
- Sensitive to beam instabilities
- The recorded signal is proportional to the first derivative of the phase term ($\nabla\Phi(x,y)$)
- Adequate to study cartilages, joints, samples with wide variation of refractive intex

Elettra Sincrotrone Trieste

Interferometry: from phase shift to image contrast

- Interferometry is a family of techniques in which waves are superimposed in order to extract information.
  - Widely used in optics (visible light)
  - It can be used in X-ray phase contrast imaging to transform the phase shift introduced by the object into image contrast
- Two different interferometric approaches:
  - Crystal interferometry (Bonse and Hart, 1965)
  - Grating interferometry (David et al, 2002; Momose et al., 2003)

Bonse, U. and Hart, M. (1965). Appl. Phys. Lett. ***6****, 155–156.*
David, C., Nöhammer, B. et al. (2002). Appl. Phys. Lett. 81, 3287–3289
Momose, A. et al. (2003). Japan J. Appl. Phys.: 2 Lett. 42, L866– L868

X-ray interferometry with crystals

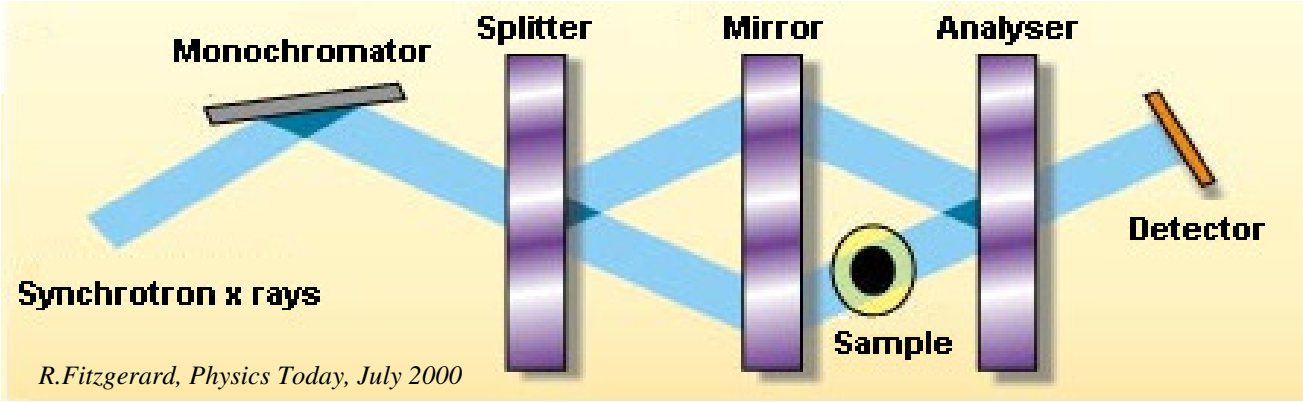

- The method has been pioneered by U.Bonse and M.Hart. A.Momose, T.Takeda et al. have refined the technique for medical applications.
- the I crystal splits the monochromatic beam into two beams with the same phase
- II crystal acts as a mirror
- III crystal recombines the two beams
- A phase shift on the probe beam is produced by the presence of the sample
- The beams re-combinated at the analyzer position generate an interference pattern registered by the detector
- Access to $\Phi(x,y)$
- Using monolithic Si crystal the limitation of the technique concerns the maximum size of samples to be studied. Interferometers based on double crystal systems are very sensitive to vibrations and require very accurate alignment systems: this limit their applications for imaging purposes.

Refs.: U.Bonse, M.Hart, Appl.Phys.Lett. 6,1965; A.Momose et al:, NIMA 352, 1995, A.Momose et al.: Opt. Express 11 2003, A. Momose et al., Japan J. Appl. Phys. 44, 2005

Grating interferometric imaging (GI)

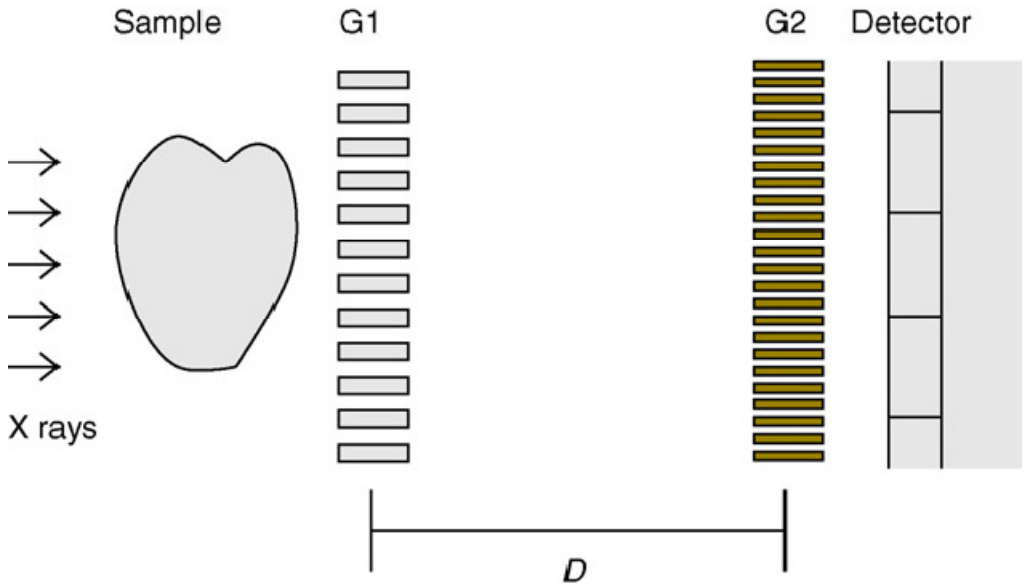

Based on an optical phenomenon discovered by Talbot (1936) and explained by Rayleigh (1881).

With a coherent radiation, the image of the grating is repeated at regular distances behind the grating, $D = 2d^2/\lambda$ (d=grating period, λ=wavelength).

The X-ray wavefront transmitted by the sample go through a **linear diffraction grating G1** (*beam splitter*). Downstream G1, a pattern of interference fringes is formed. The local distortions of the fringe pattern from its ideal regular shape contain information on the sample structure. Since the fringes are too closely spaced to be resolved by the pixel detector, **an additional absorption grid** (**G2**, called *analyzer*) in front of the detector is needed to transform fringe-position information into intensity values on the detector.
A modified set-up can be applied to polychromatic spectrum from an X-ray tube.

T. J. Davis et al., Phys. Rev. Lett. 74, (1995), A.Momose et al.: Opt. Express 11, 2003, Weitkamp, T., et al., Opt. Express, 13(16), 2005, Weitkamp T et al, Eur. J. Radiol. 68, 2008

Grating Interferometry- Limitations

Demanding mechanical requirements (precision ~ 20-30 nm)

- Field of view must be increased to clinical size
- At the moment 5 cm x 5 cm

Limited exploitation of X-ray output

- 20% - 30% due to source grating
- grating silicon substrates (~ 300 μm)

Long exposure time and high delivered dose

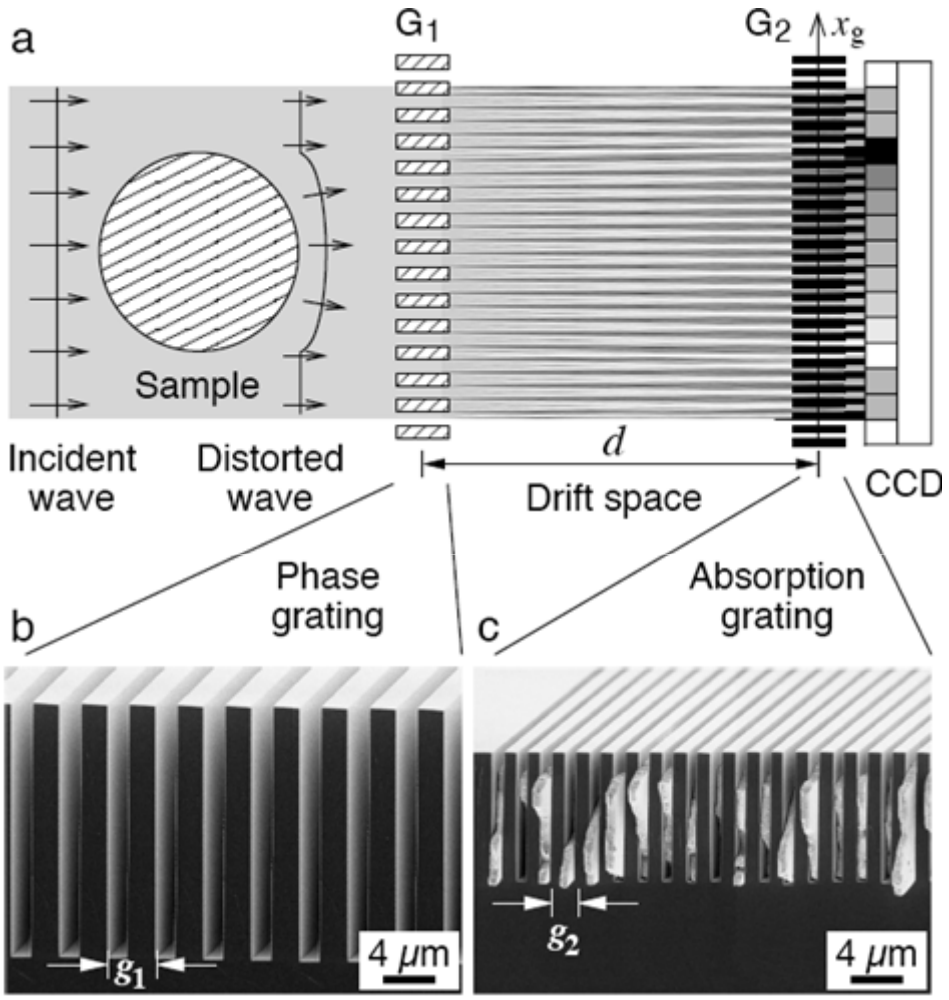

Grating non-interferometric imaging: Coded apertures method

Principle

The phase sensitivity of an imaging system can be strongly enhanced by illuminating only the edge of the active surface of the detector pixel.

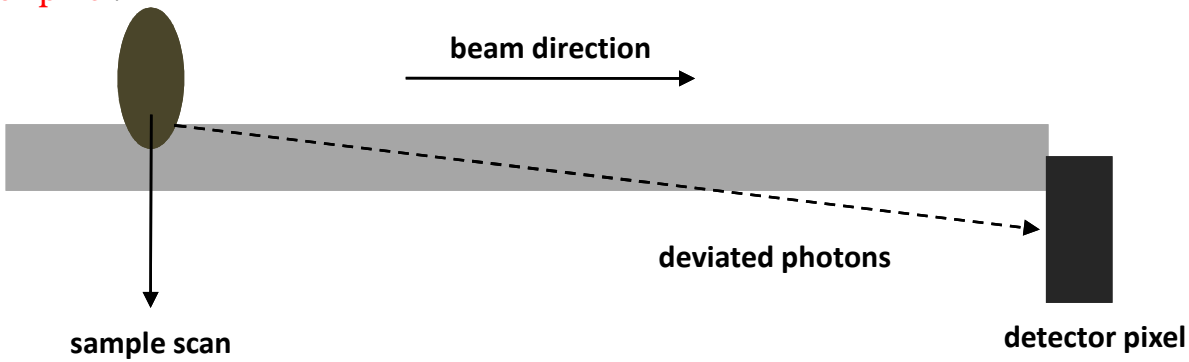

X-rays normally not hitting the detector active surface can be deviated inside it, increasing the number of counts.

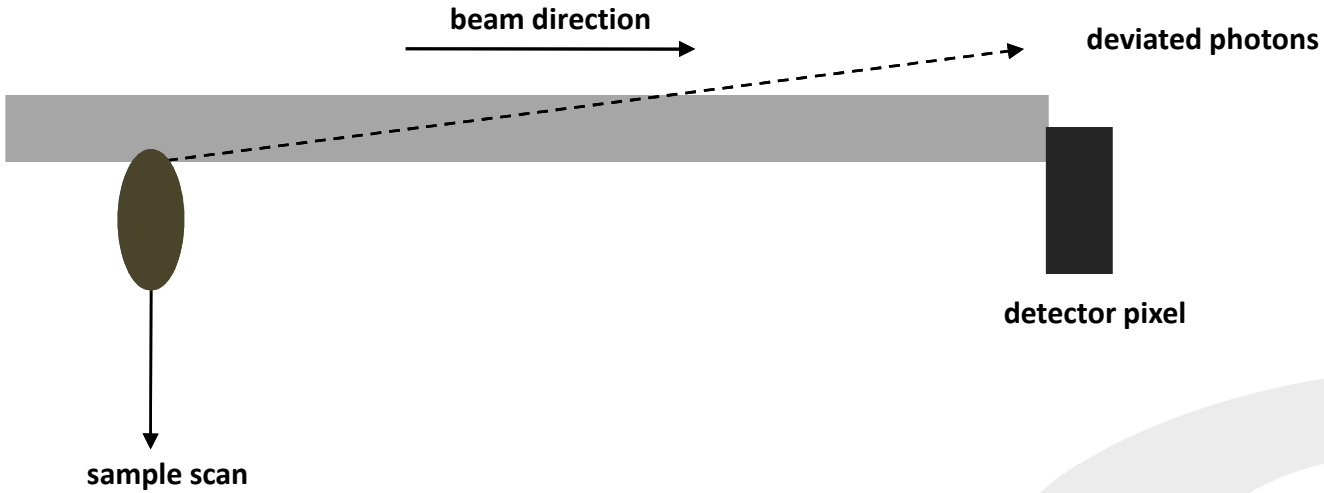

X-rays originally hitting the detector active surface can be deviated outside it, thus decreasing the number of counts.

Grating non-interferometric imaging: coded-aperture method

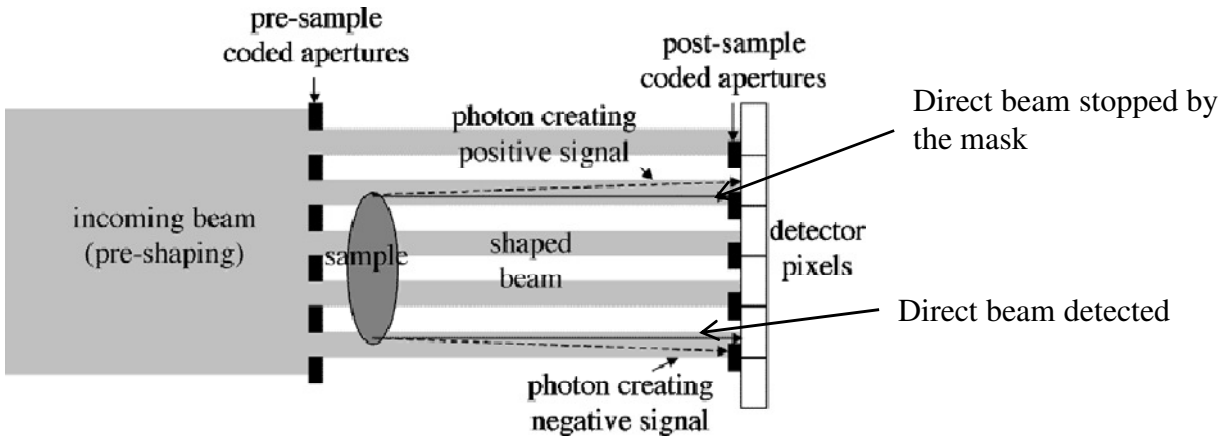

- ✓ the detector is divided by a mask ('detector mask') into a pattern of sensitive and insensitive regions between adjacent pixels, and a pre-sample mask creates the same pattern of beams that impinges on the boundaries of sensitive and insensitive regions.
- ✓ The beams are deviated by refraction in the sample, resulting in intensity variation at the detector.
- ✓ The pre-sample coded-aperture system ('sample mask') is placed immediately before the sample, and it creates an array of individual beams each one impinging on the edge of the detector pixels, as defined by the detector mask.
- ✓ the pre-sample mask prevents unnecessary radiation from transversing the sample, thus ensuring efficient dose delivery.
- ✓ It can be applied to polychromatic radiation from an x-ray tube

Olivo A et al., Med. Phys. ***28****, 2001, Olivo A and Speller R, Appl. Phys. Lett. 91, 2007*

SYRMEP layout for PHC imaging

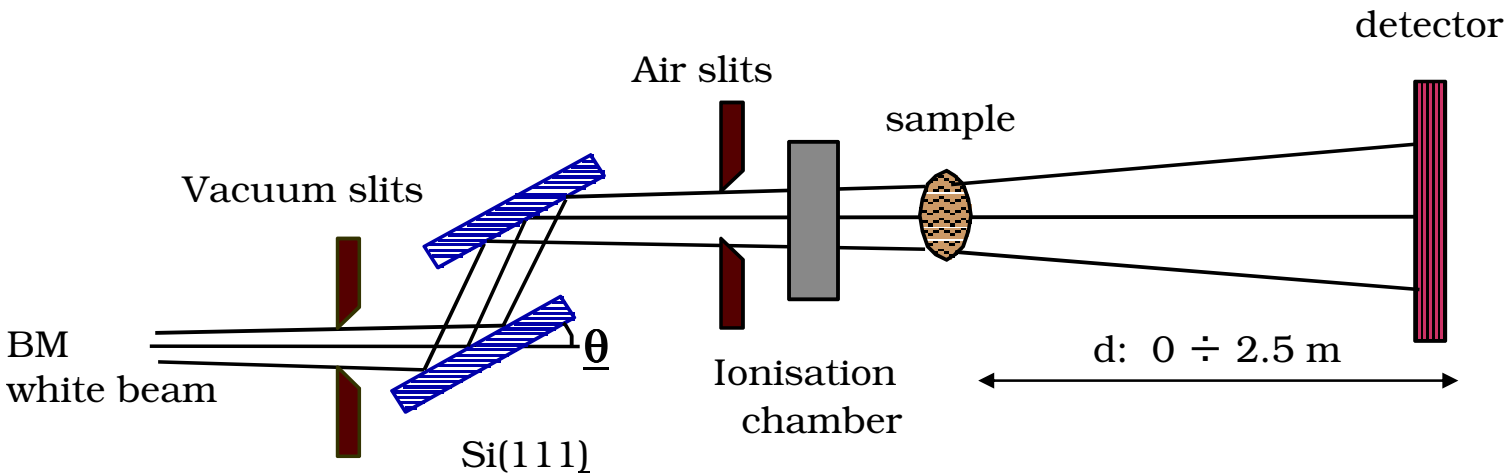

Front-end horiz.
acceptance: 7 mrad

ABI setup

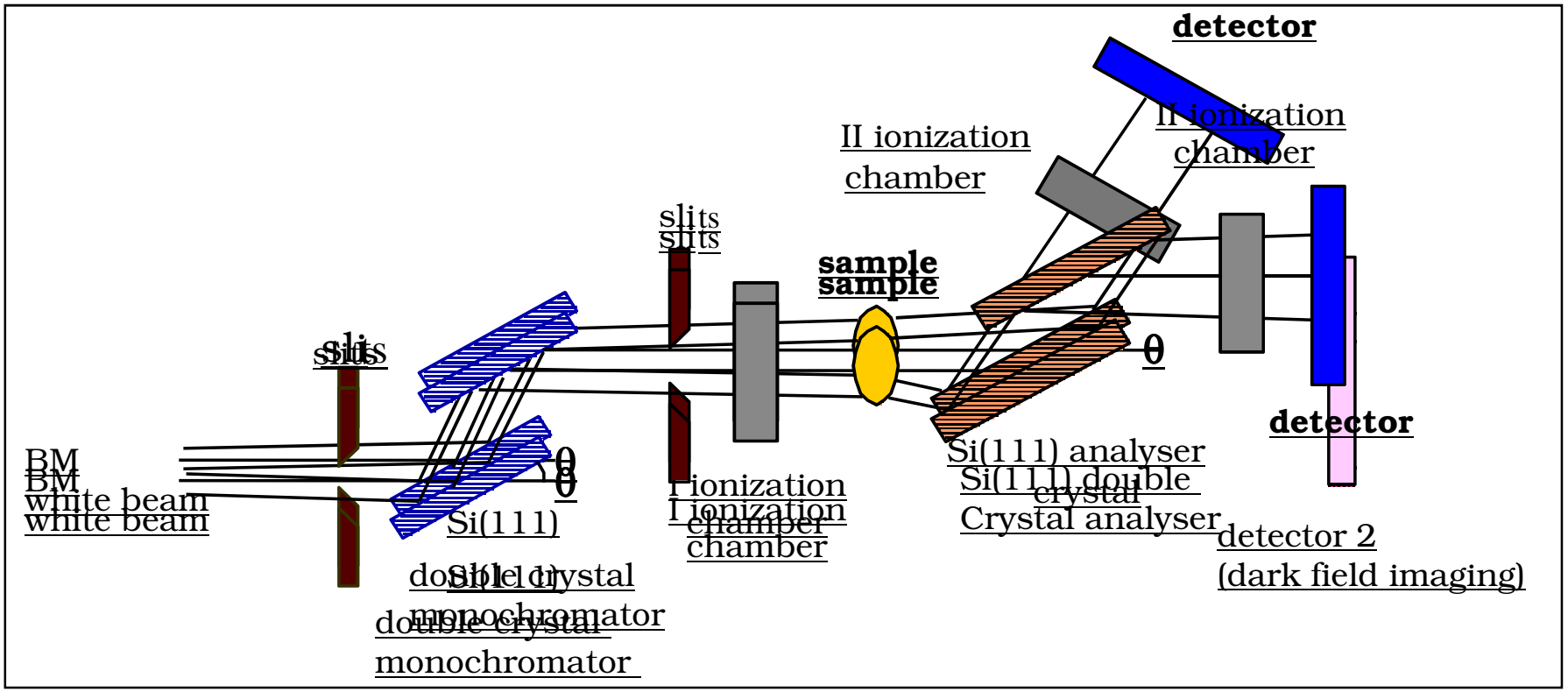
detector
II ionization chamber
II ionization chamber
slits
slits
sample
sample
slits
slits
θ
θ
θ
BM
BM
white beam
white beam
Si(111)
double crystal
monochromator
Si(111)
double crystal
monochromator
I ionization chamber
I ionization chamber
Si(111) analyser
Si(111) double crystal
Crystal analyser
detector
detector 2
(dark field imaging)

ABI images for different analyzer positions

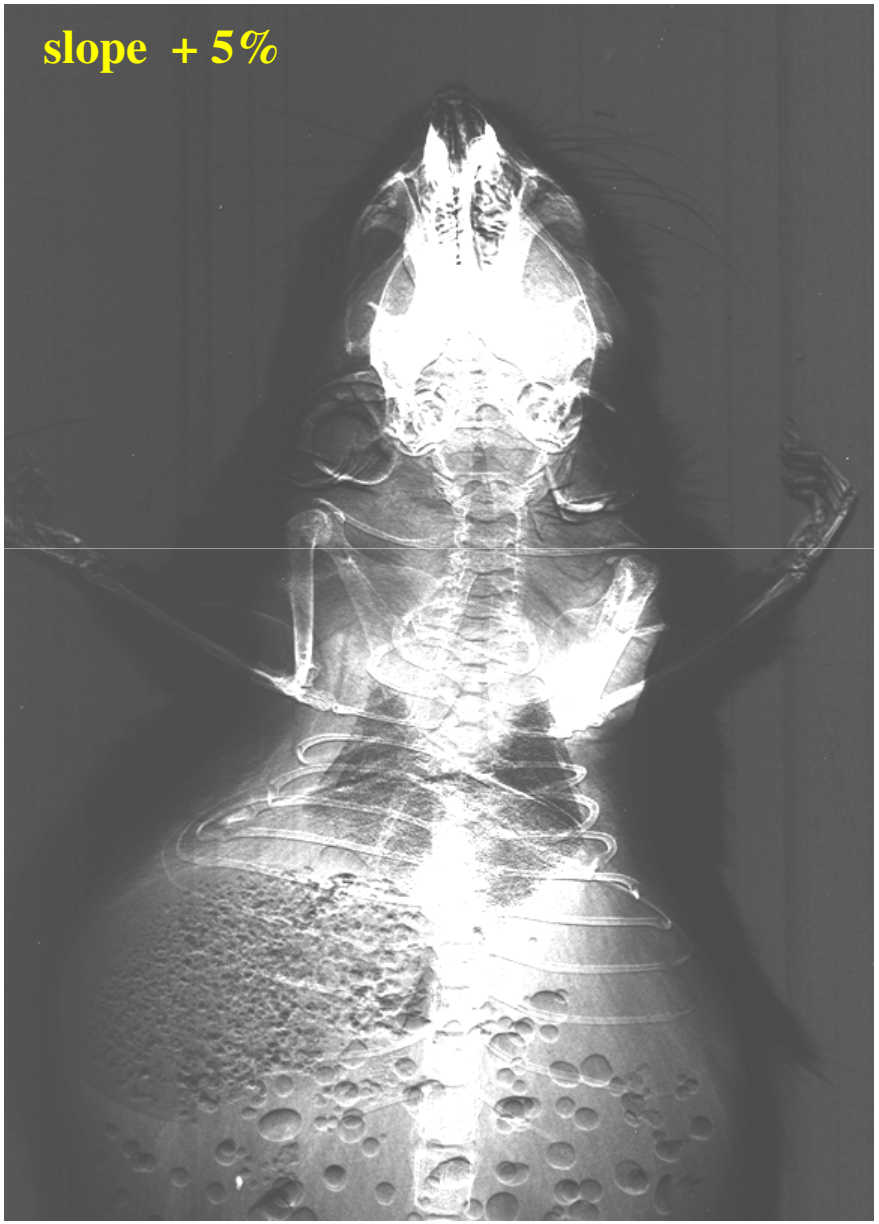

Elettra Sincrotrone Trieste

Images obtained from application of the algorithm

Apparent absorption

Refraction image

Elettra Sincrotrone Trieste

Breast imaging

Techniques: PHC, planar imaging for patients protocol

DEI, planar and CT for *in-vitro* imaging

Breast imaging – first protocol with patients at Elettra

Agreement among the Public Hospital of Trieste, the University of Trieste and Elettra

Aim: Explore the potential of phase contrast imaging on selected cases

Target: Patients whose conventional diagnosis gave uncertain results.

Modality:
I) PHC radiography with film systems
II) PHC imaging with digital detectors
III) Tomo-mammography (X-ray energy > 30 keV)

Projection imaging
X-ray energy: 17– 22 keV

Outcomes from the first protocol (I, II)

SR exams have:
- higher specificity,
- better agreement with the golden standard (biopsy),
- improved image quality,
- strong reduction of delivered doses.

Elettra Sincrotrone Trieste

Clinical Mammography

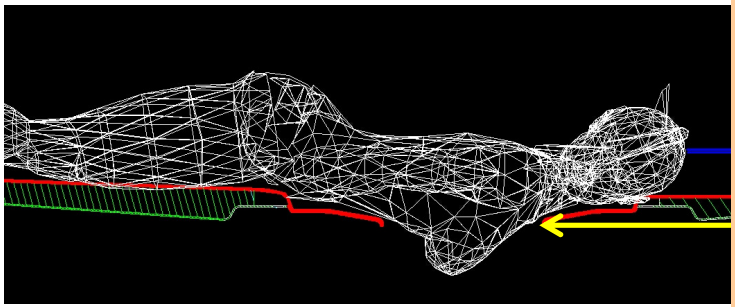

Outcomes of first protocol

Images with SR have:

- *higher specificity,*
- *better agreement with the golden standard (biopsy),*
- *improved image quality,*
- *strong reduction of X-ray doses.*

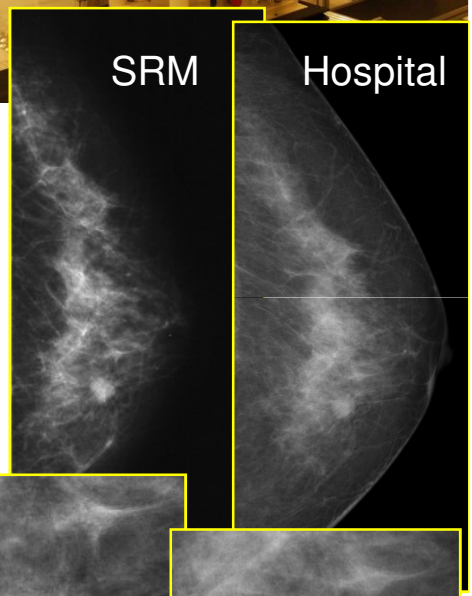

Next step: Low dose phase contrast breast CT

PiXirad Chromatic Photon Counting

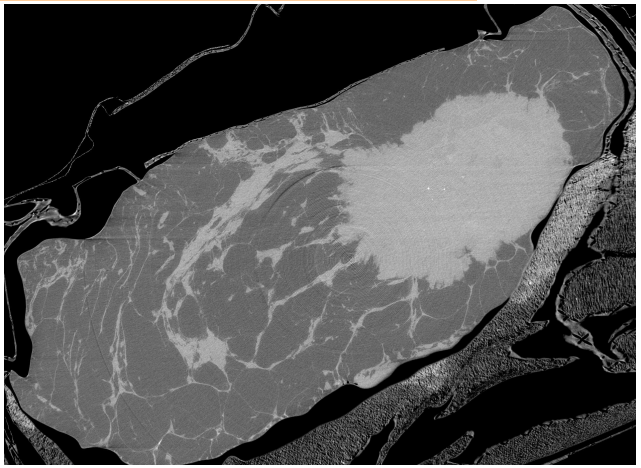

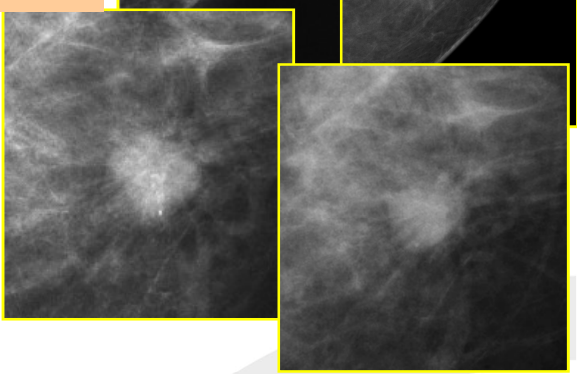

CSIRO THE UNIVERSITY OF MELBOURNE UNIVERSITÄTSMEDIZIN GÖTTINGEN UMG

Computed μ-Tomography (μCT)

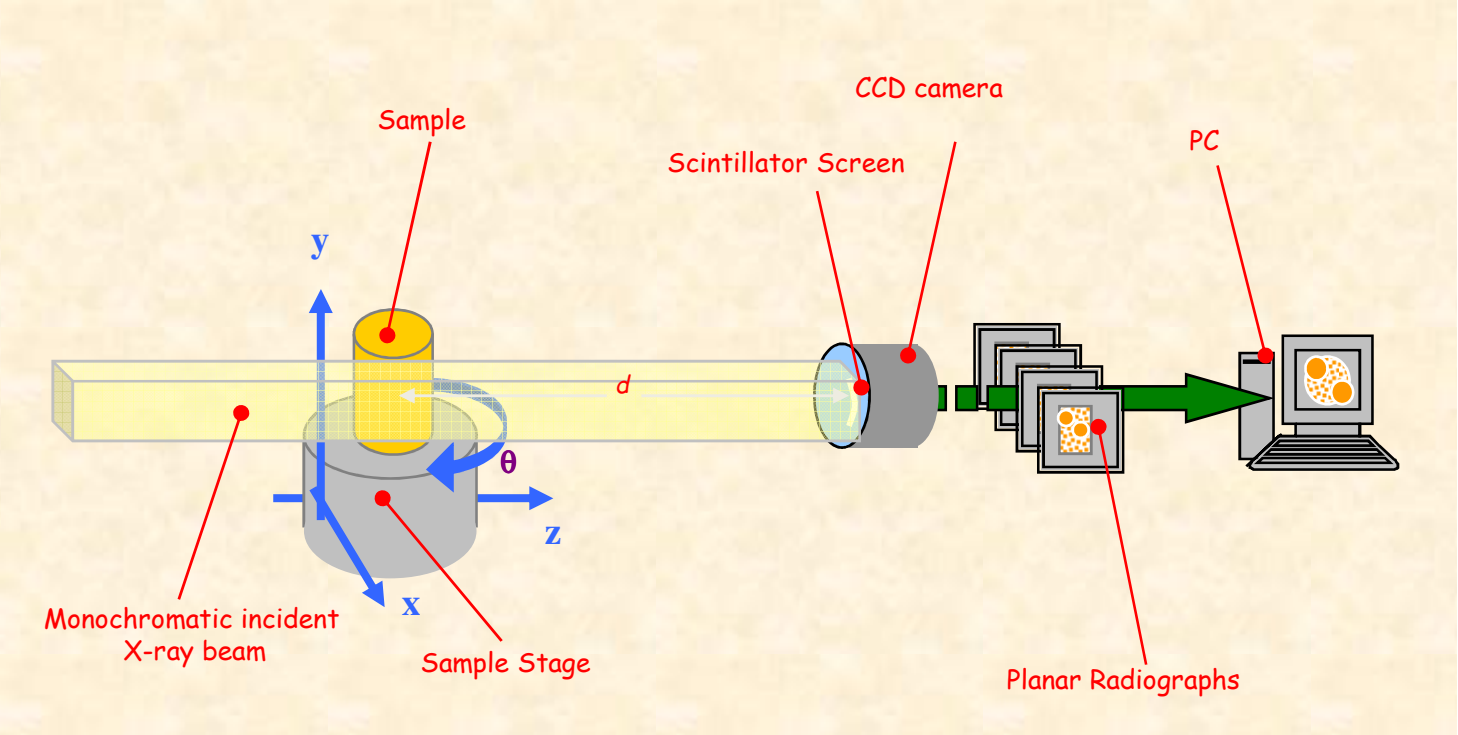

- *not destructive tool* to study the ***internal structure*** of any kind of sample
- no sample preparation
- it gives access to quantitative information on the *density maps* of the irradiated volumes
- suited for *in vivo* imaging of small animals

Elettra Sincrotrone Trieste

Potentials of ABI

In vitro studies:

- Studies of cartilages and bones interfaces

- Imaging of finger joints

ABI studies of Cartilage and bone interface

Osteoarthrosis (OA) is a disease characterized by the progressive degeneration of articular cartilage and the development of altered joint congruency. It has a high incidence in the adult population. Affecting mainly the elderly population, it is one of the main causes of disability worldwide. Conventional radiography detects only **important osseous changes**, at advanced OA or RA stages, when therapeutic strategies are less effective. **Early changes** in the **cartilage** and other **articular tissues** are **not** directly visible. MRI imaging works better but the maximum achievable spatial resolution is not always adequate.

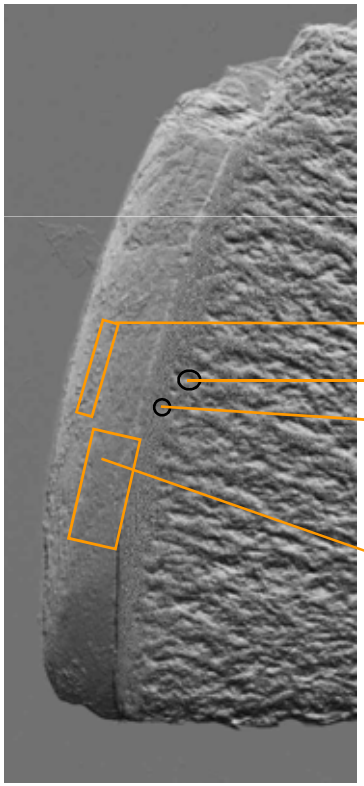

Need to study:
- cartilage
- cartilage-bone interfaces
- changes in the bone structure

Superficial Layer (Zone of horizontal collagen fibers with flat cells)

Subchondral Bone Plate (**Important for diagnostic purposes in OA**)

Tidemark (Border between normal and mineralized cartilage)

Transitional and Deep Layer (round cells, collagen fiber switches from horizontal to vertical orientation, increasing stiffness and material density)

Aim: detect the architectural arrangement of collagen within cartilage and evaluate how the cartilage degeneration affects the underlying subchondral and trabecular bone.

Femur head core cuts: collagen arcades structure

- The ABI technique allows to visualize the discontinuities in the sample and the inner structures invisibles by means of conventional X-Ray imaging.
- The transition bone-cartilage is emphasized.
- The articular cartilage striations are well visible due to X-ray diffraction at edges of fibers

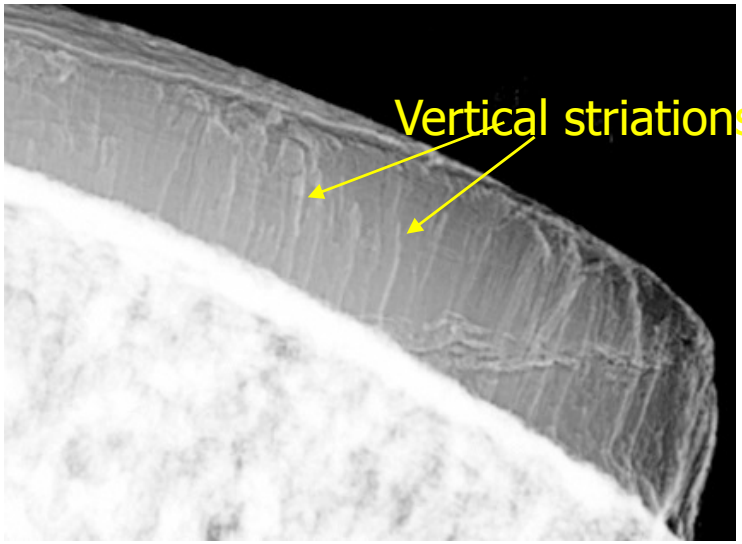

Apparent absorption image

Refraction image

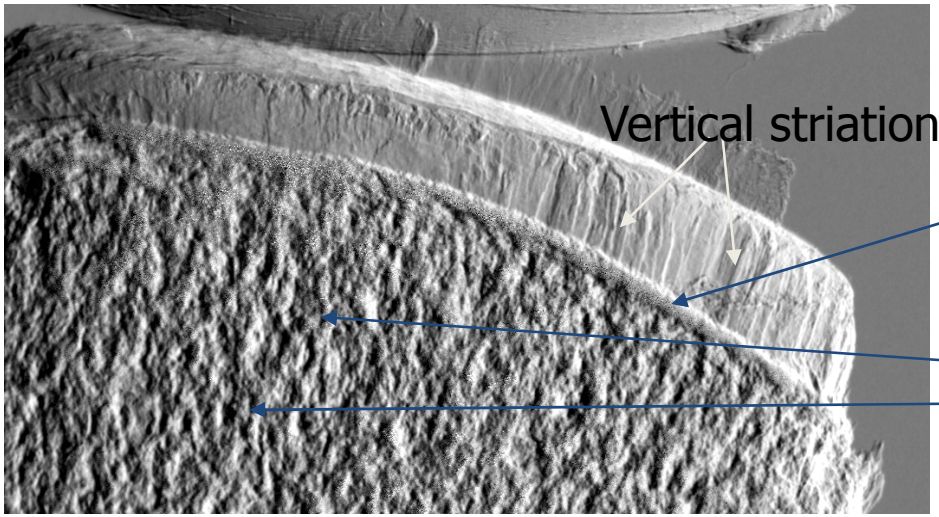

Elettra
25 keV

Muehleman C, Majumdar S, Issever AS, Arfelli F, Menk RH, Rigon L, Heitner G, Reime B, Metge J, Wagner A, Kuettner KE, Mollenhauer J, Osteoarthritis and Cartilage 12 (2): 97-105 FEB 2004

Femur head core cuts: comparison with MRI

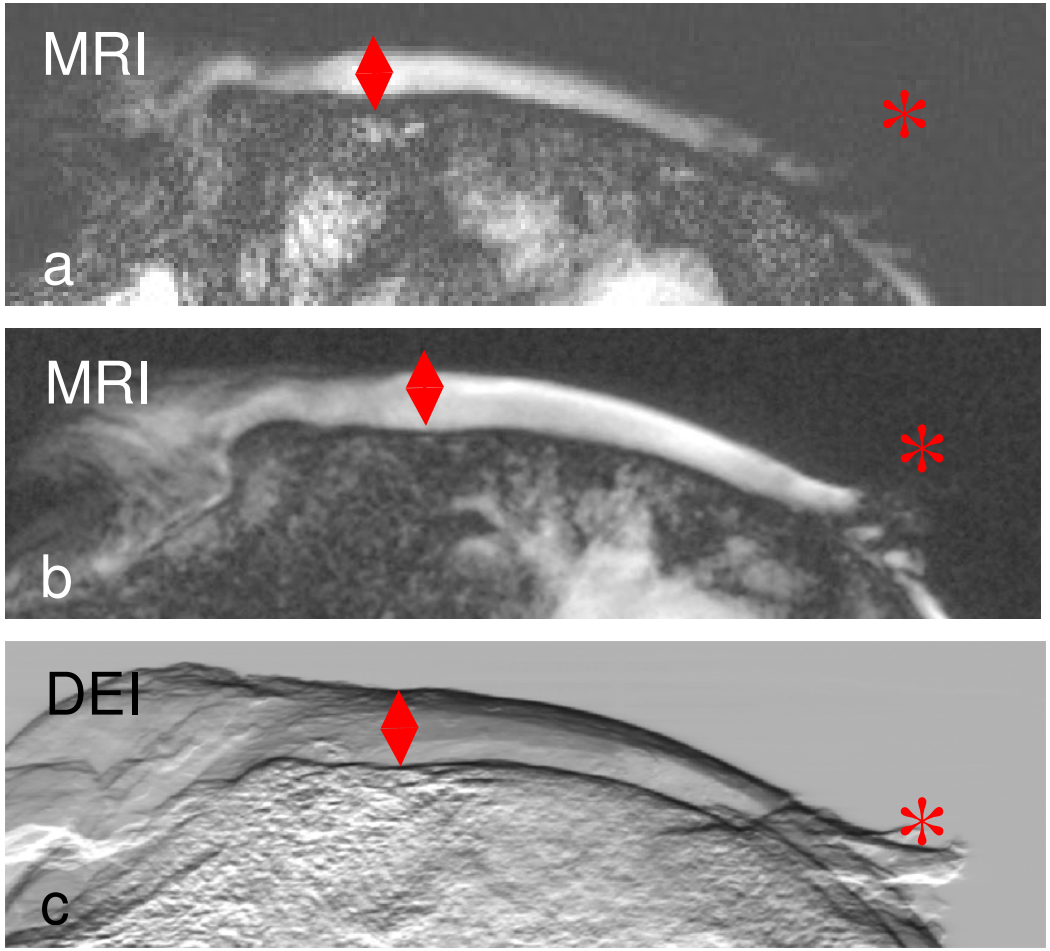

5 sec

150 sec

A Wagner, M Aurich, N Sieber, M Stoessel, WD Wetzel, K Schmuck , M Lohmann, B Reime, J Metge, P Coan, A Bravin, F Arfelli, L Rigon, RH Menk, G Heitner, T Irving, Z Zhong, C Muehleman, J A Mollenhauer sumbitted to NIM A

ABI studies of the finger joint

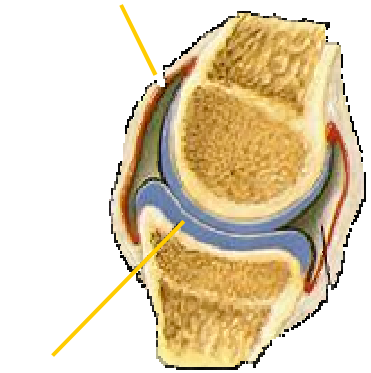

Conventional radiograph

Apparent absorption image @ 20 keV
at ELETTRA

Lewis, R. A., et al., British J. Rad., 76(905), 301-308 (2003)

Index finger proximal interphalangeal joint

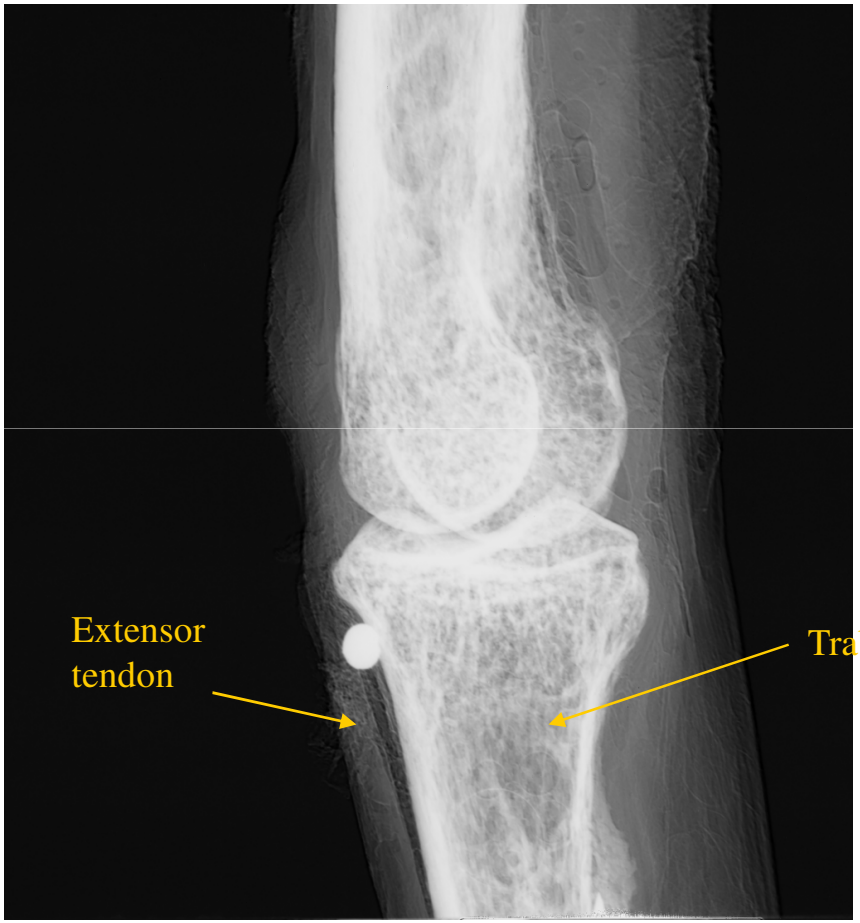

Apparent absorption Image

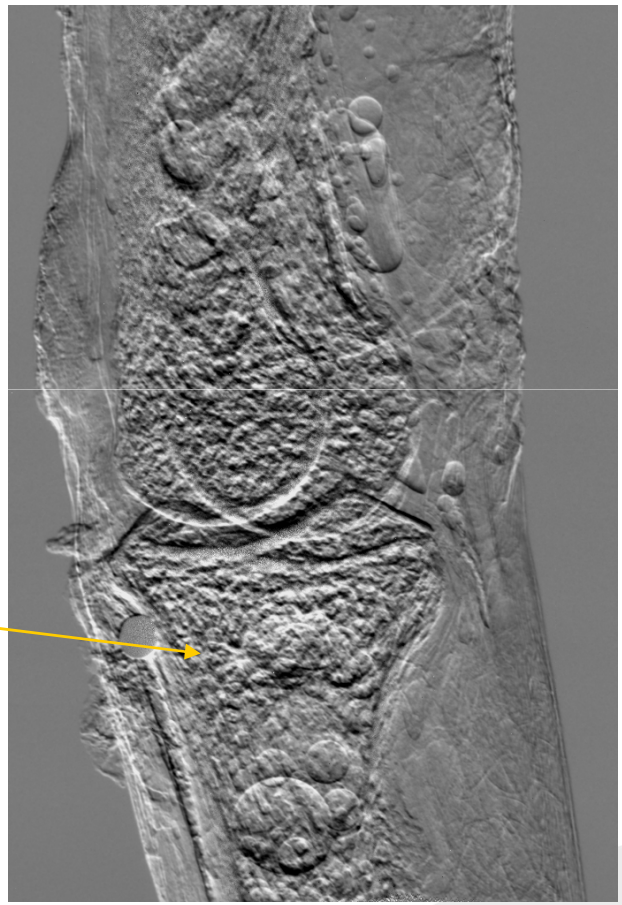

Refraction Image

Lewis, R. A., et al., British J. Rad., 76(905), 301-308 (2003)

Index finger proximal interphalangeal joint

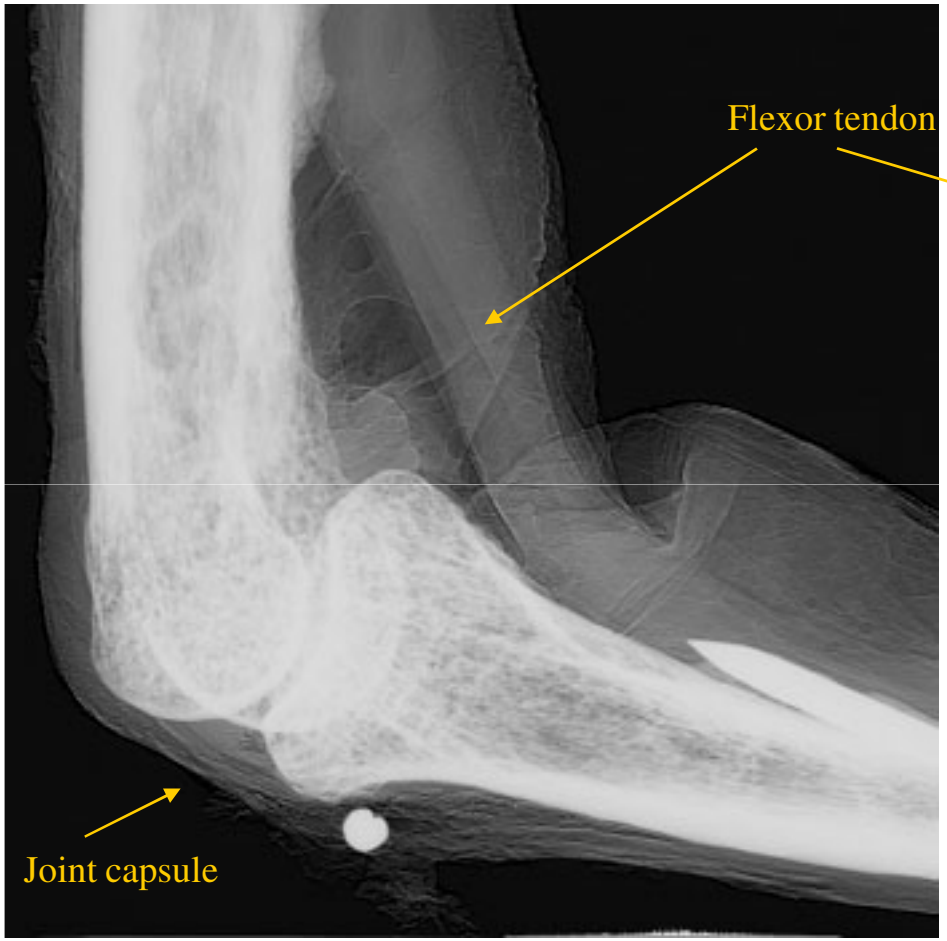

Apparent absorption Image

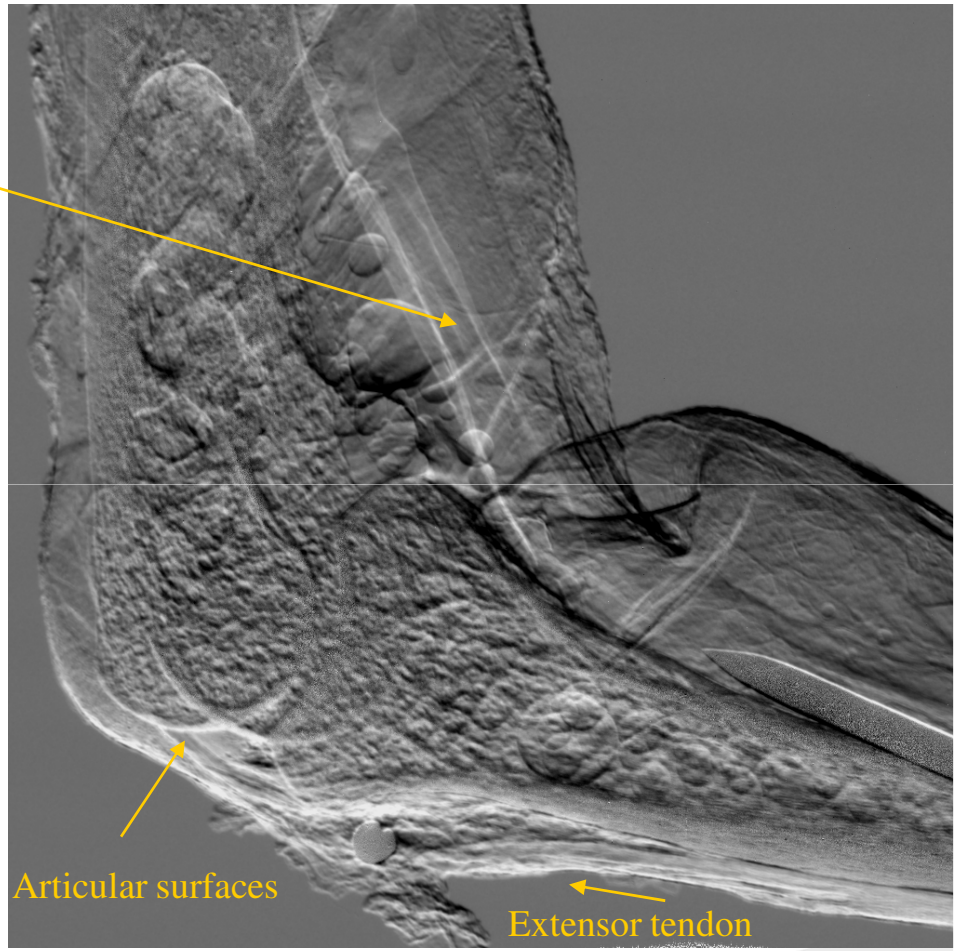

Refraction Image

Lewis, R. A., et al., British J. Rad., 76(905), 301-308 (2003)

Elettra Sincrotrone Trieste

Lungs imaging

Technique: Propagation Based

+ contrast agent (Barium)

Modalities: micro-CT *ex-vivo* images on mice

planar for *in-vivo* images on rabbits

- Cell tracking technique
- Use of phase retrieval to increase the tissue differentiation and allow quantitative analysis

Imaging of asthmatic mice – feasibility study

Animal model of allergic asthma induced by ovalbumin based on balb/c mice developed by CBM in collaboration with the University of Wien.

Aim: evaluate the potential of SR-based technique for **functional** and **morphologic** imaging of mice lungs

Available techniques: optical imaging and PHC micro-CT

Linköping University

Programme on Scientific and Technological Cooperation between Italy and Sweden financed by Ministero degli Esteri

Imaging protocol: use of macrophages with double staining

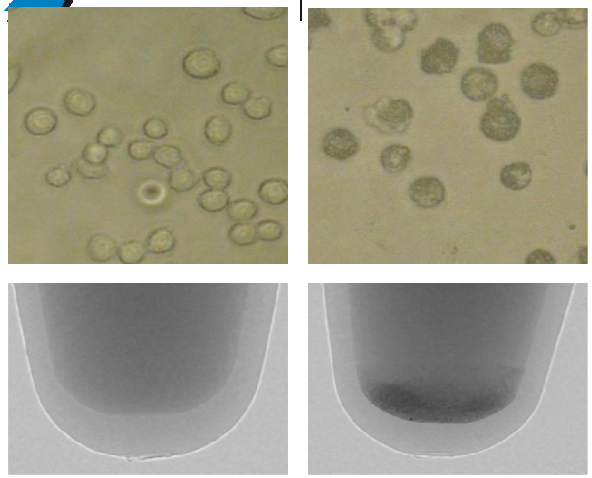

Unlabeled macrophages

Macrophages labeled with Ba

Use of immortalized Murine Alveolar Macrophage Cell line with double staining:
- Barium sulfate (clinical contrast agent Micropaque CT (Guerbet, F))
-DiD fluorescent dye to be used for cells localization inside the lungs using fluorescence microscopy.

Macrophages were adminstered intra tracheally 48 hours after asthma induction

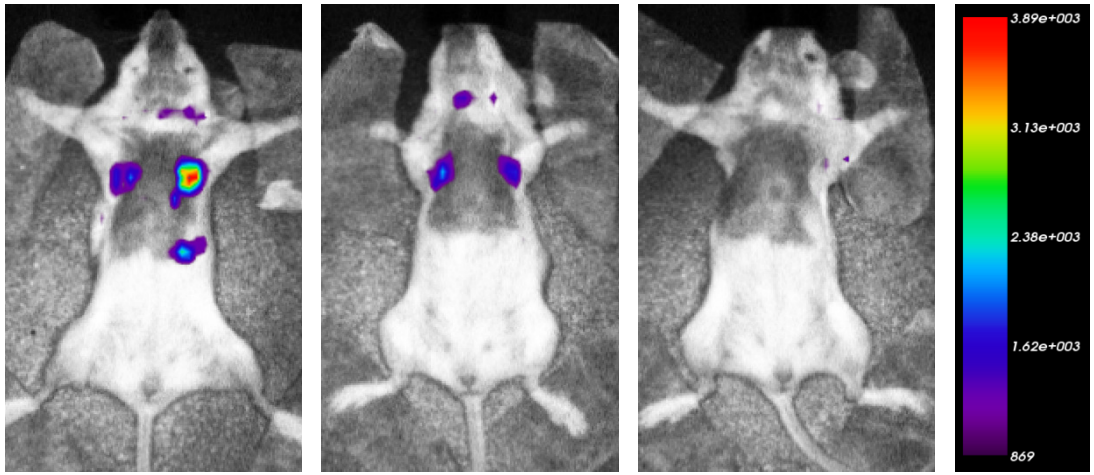

Asthmatic mouse treated with macrophages

Normal mouse treated with macrophages

Native mouse untreated

In vivo validation of homing of the macrophages to inflammation sites. Images performed 24 hours after macrophages administration.

Elettra Sincrotrone Trieste

Reconstructed slice –

Filtered back projection standard reconstruction procedure

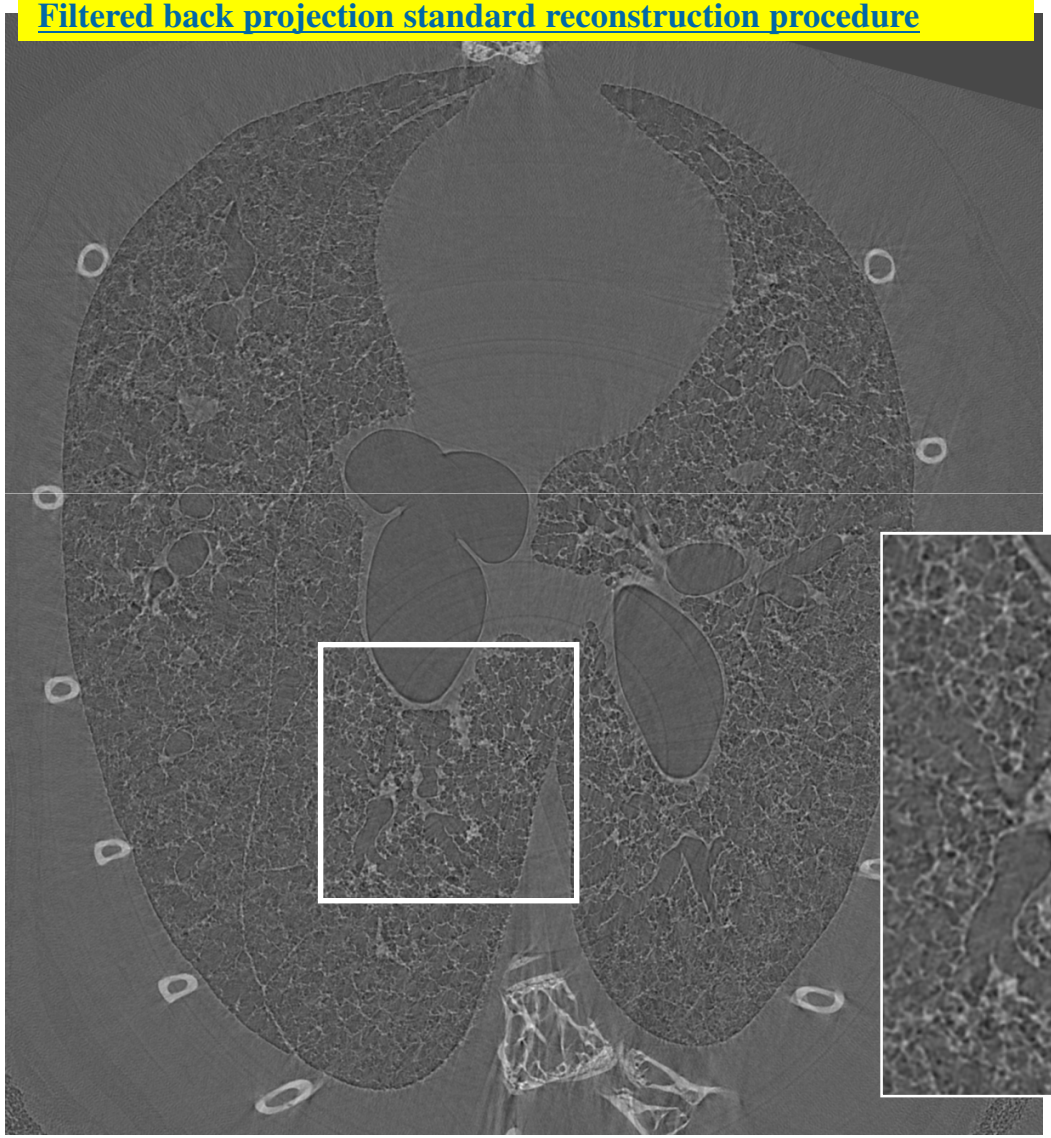

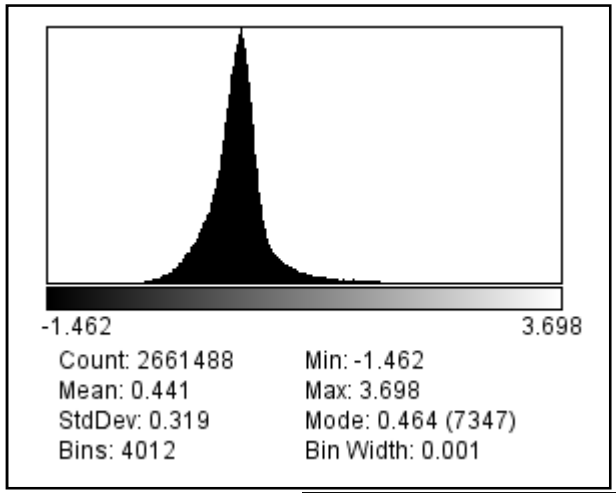

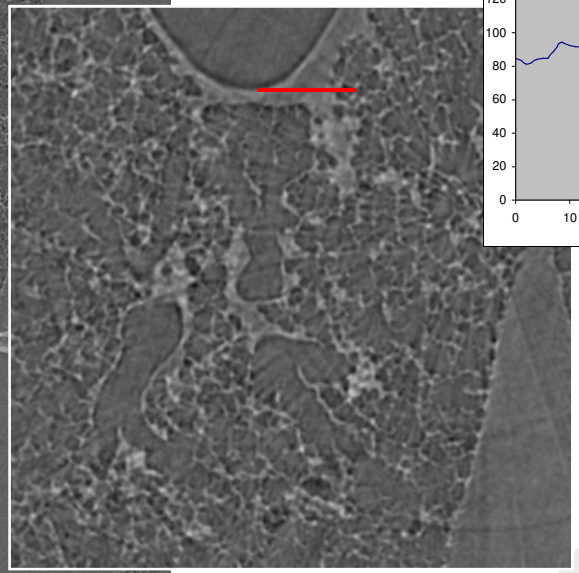

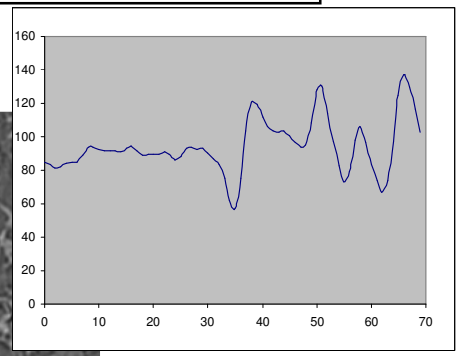

Typical edge enhancement effects due to phase contrast

Elettra Sincrotrone Trieste

Visualizing Barium brought by macrophages into the inflammation sites

Sample: acute asthma mouse treated with macrophages labeled with Barium

Phase Retrieval pre-processing *algorithm* is applied to CT projections, (prior to the reconstruction) to enable the decoupling of *phase* from *absorption*

Assumptions (Paganin et al., 2002):
-near field phase contrast regime
- materials with δ/β = const

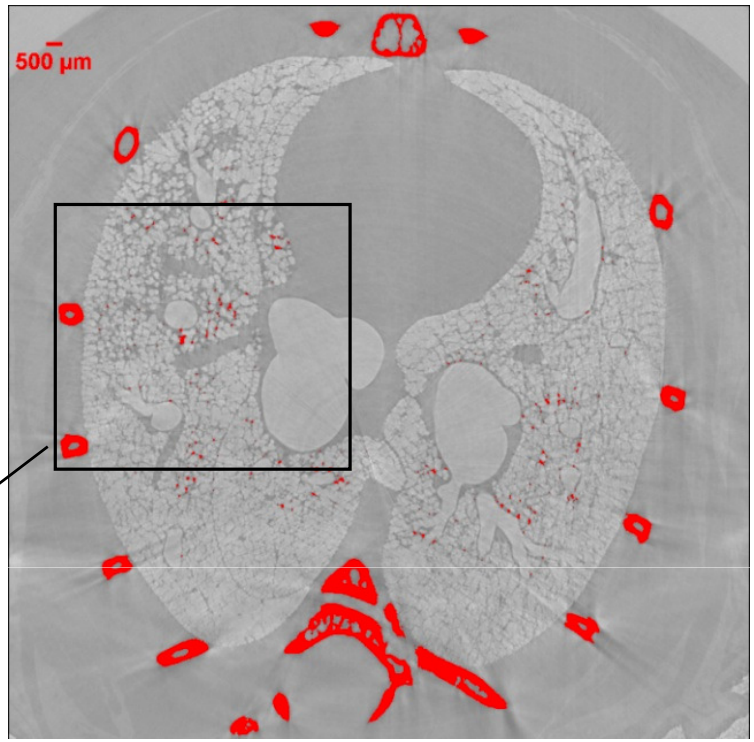

E=22 keV
PHC dist=30 cm

Bones
Barium

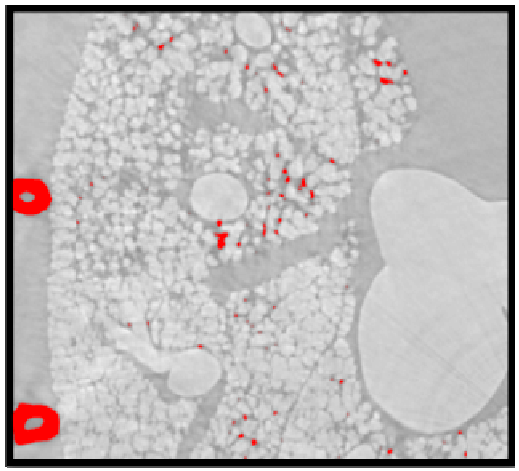

Application of Phase Retrieval for:

- Reducing the artefacts due to PHC effects around the tissue edges
- Reducing the noise
- Enhancing the phases separation

By S. Mohammadi Giuliana Tromba

Visualization of labeled macrophages

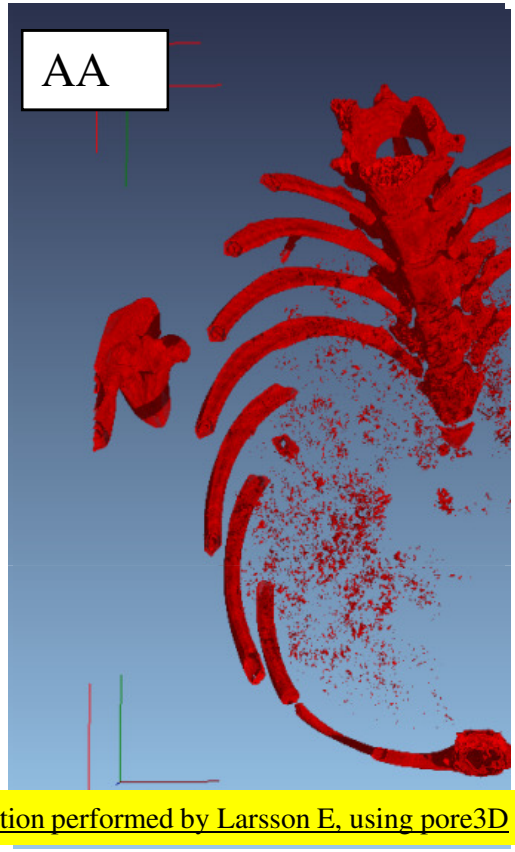

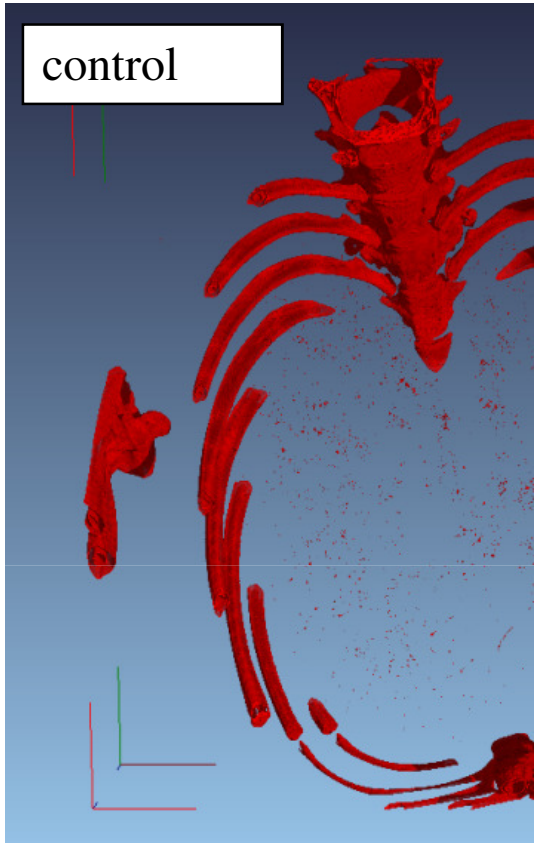

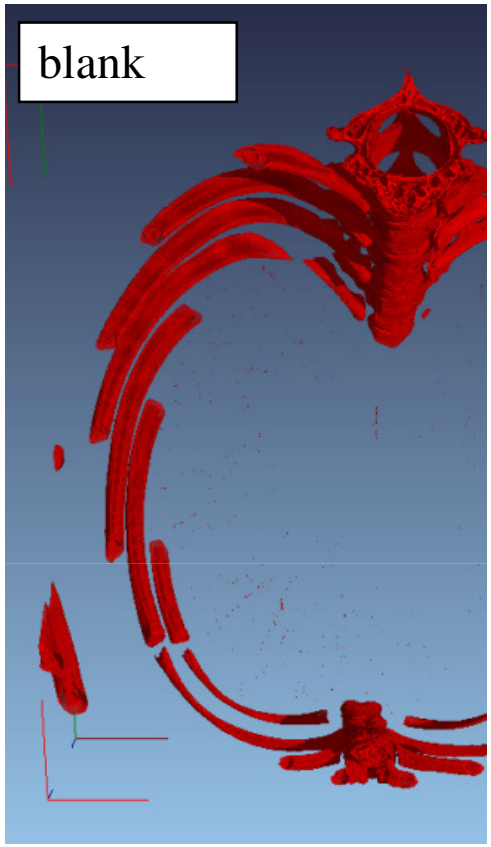

Quantification performed by Larsson E, using pore3D

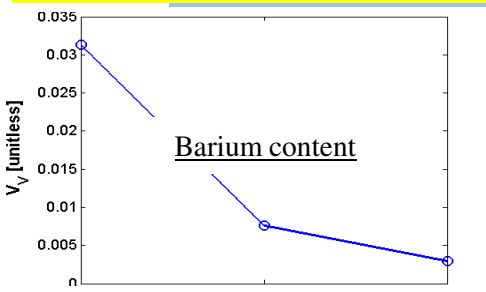

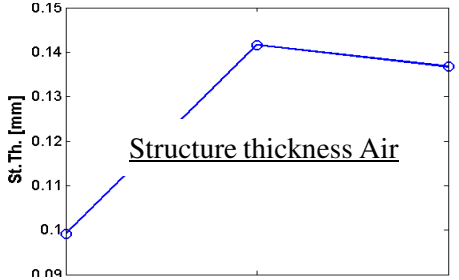

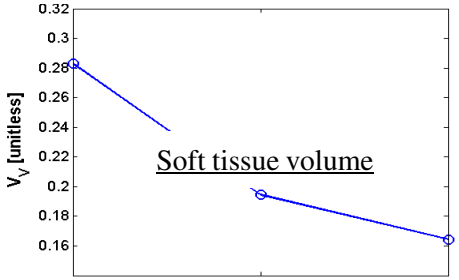

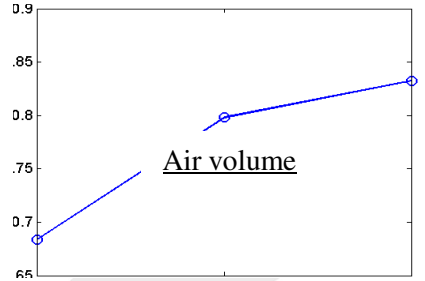

AA control blank AA control blank AA control blank AA control blank

VOI of soft lung tissue

Soft Tissue (green), Macrophages with barium (red), Medial axis/skeleton (blue)

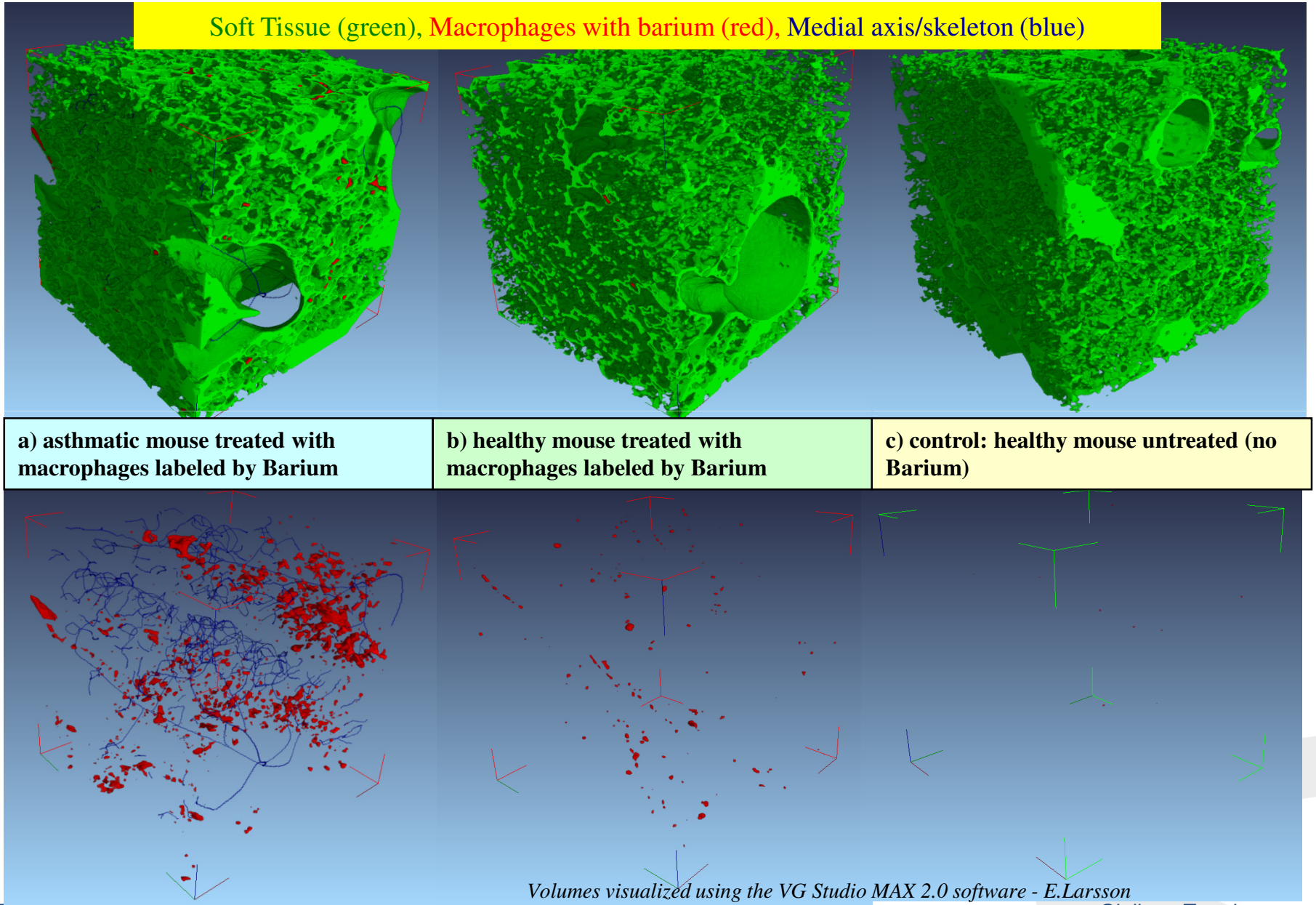

a) asthmatic mouse treated with macrophages labeled by Barium	b) healthy mouse treated with macrophages labeled by Barium	c) control: healthy mouse untreated (no Barium)

Volumes visualized using the VG Studio MAX 2.0 software - E.Larsson

Elettra Sincrotrone Trieste

In vivo studies at Spring 8 (Japan)
Effects of Ventilation on Lung Liquid Clearance at Birth

Aim: to observe lung aeration on a breath-by-breath basis.

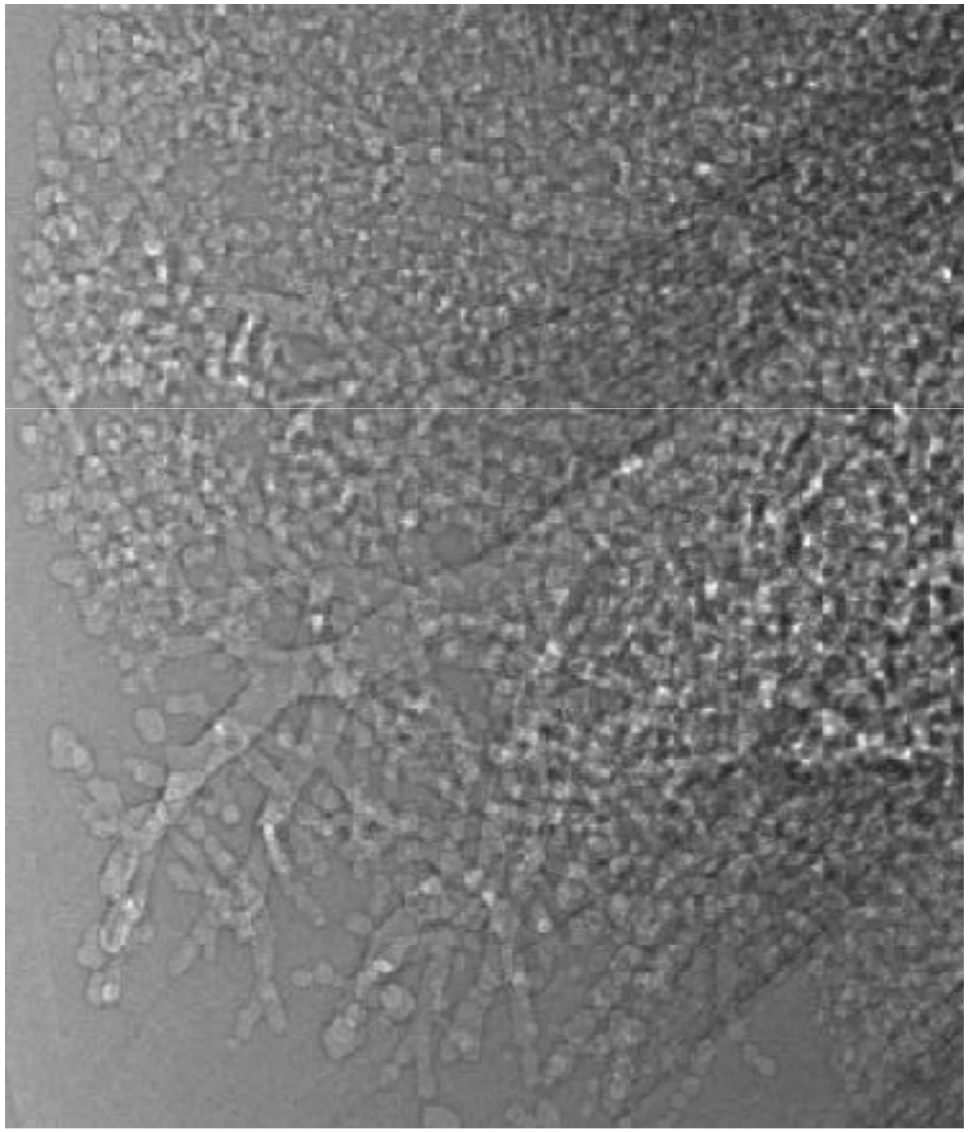

Birth: a major physiological challenge

- ✓ Clear the airways of liquid
- ✓ Entry of air generates surface tension
- ✓ Separation of the pulmonary and systemic circulations
- ✓ 10 fold increase in pulmonary blood flow
- ✓ Large increase in blood oxygenation

- ➢ Animal model: rabbit pups
- ➢ Imaged pups with phase contrast imaging (FPI), either before the first breath (fetus) and at fixed intervals after birth (up to 2h)

MONASH University Science

Courtesy of M. Kitchen, School of Physics

MONASH University
Science

X-ray imaging of the lung

Absorption Contrast

Phase Contrast, 25 keV, z=2 m

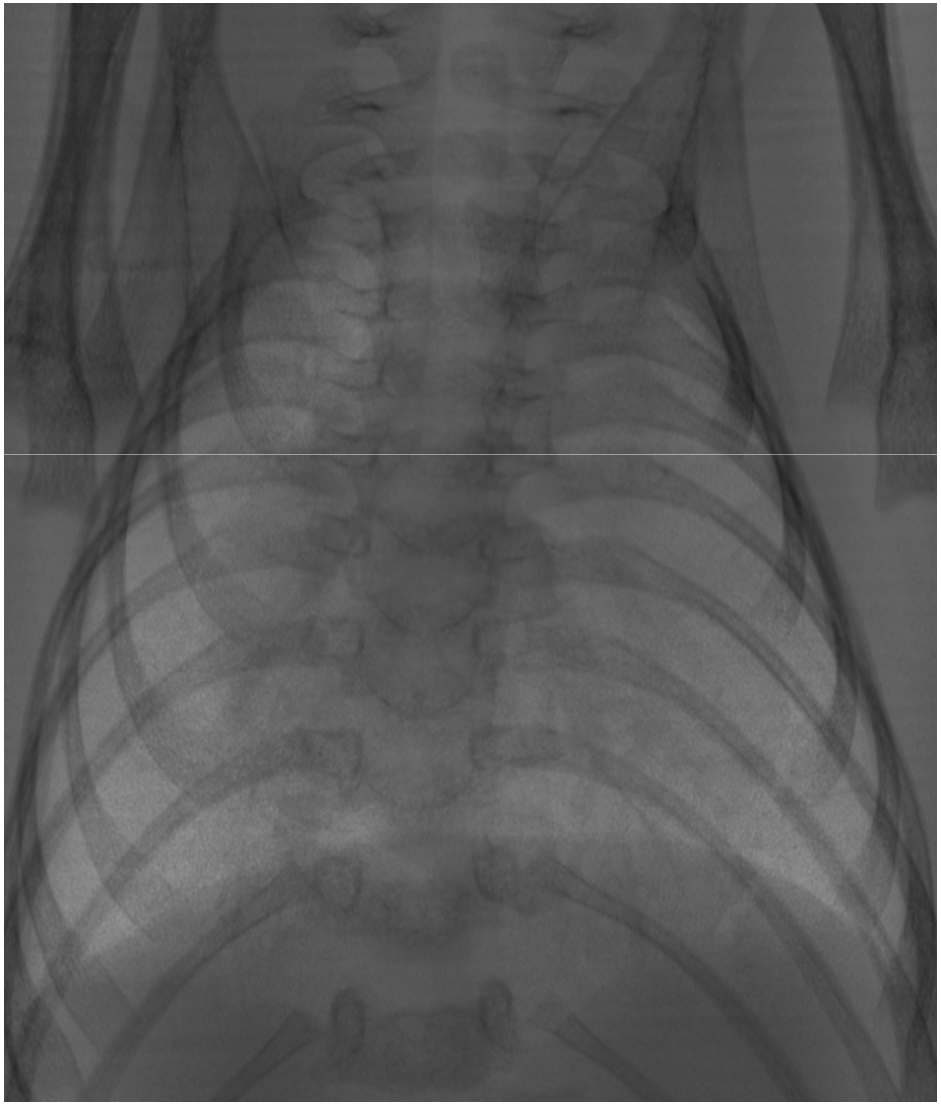

Courtesy of :M.Kitchen

Kitchen, M. J., et al., Phys. Med. Biol., 53(21), 6065-77 (2008).

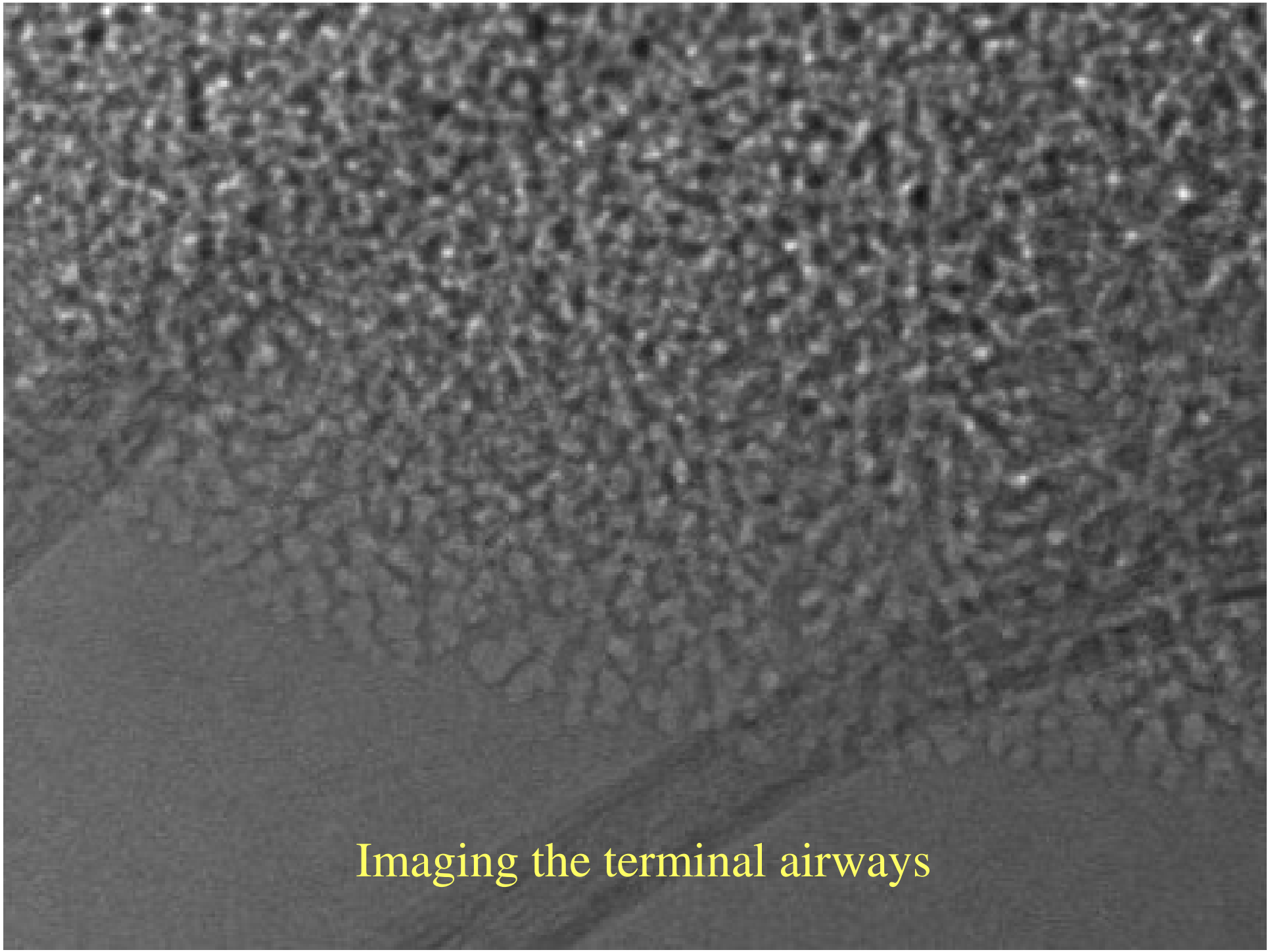
Imaging the terminal airways

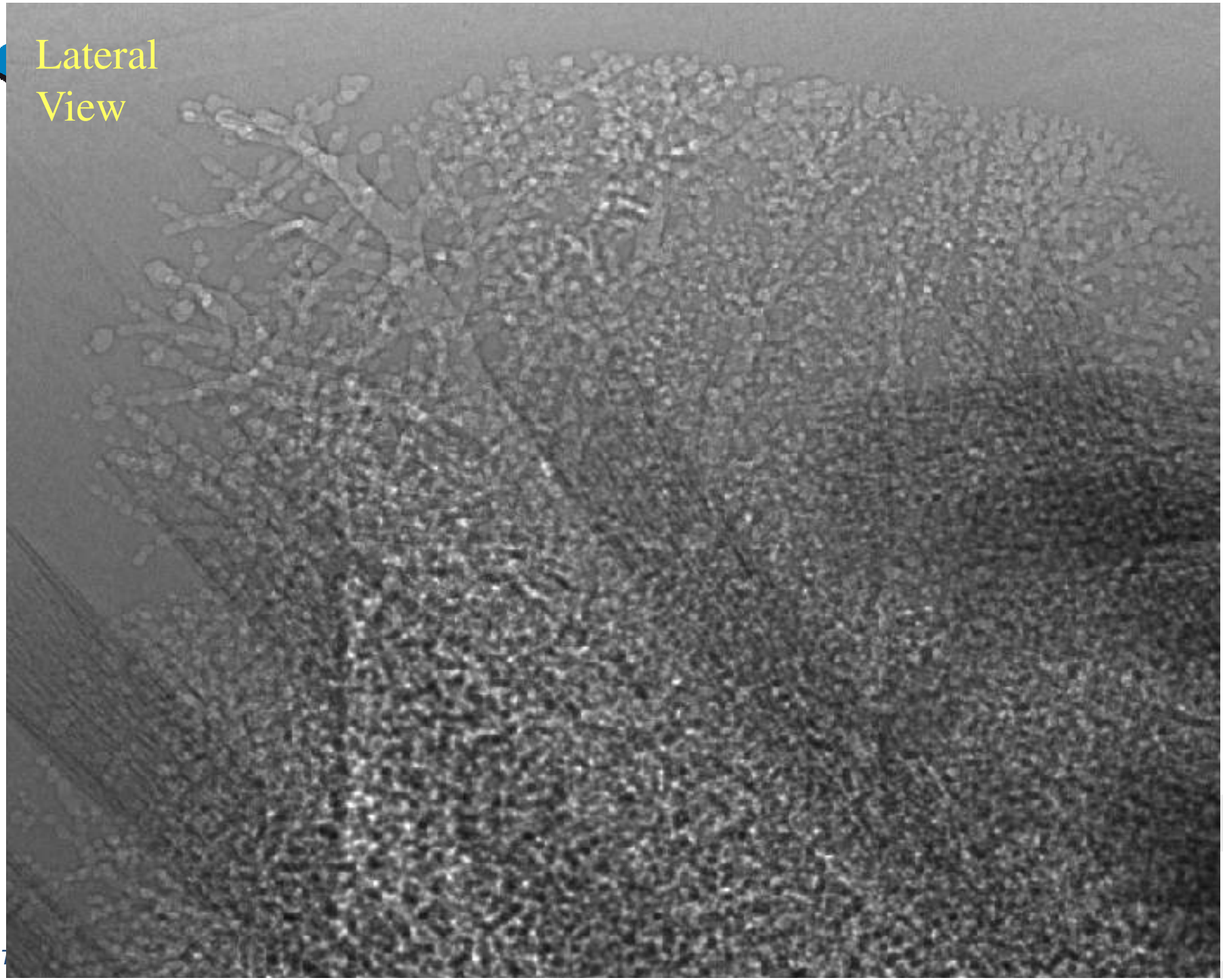
Lateral
View

Exp. time:
80 ms

Interval:
0.8 s

Skin Dose:
~ 0.15
mGy
per frame

Pixel Size:
22.5 µm

Kitchen, M. J., et al., Phys. Med. Biol., 53(21), 6065-77 (2008).

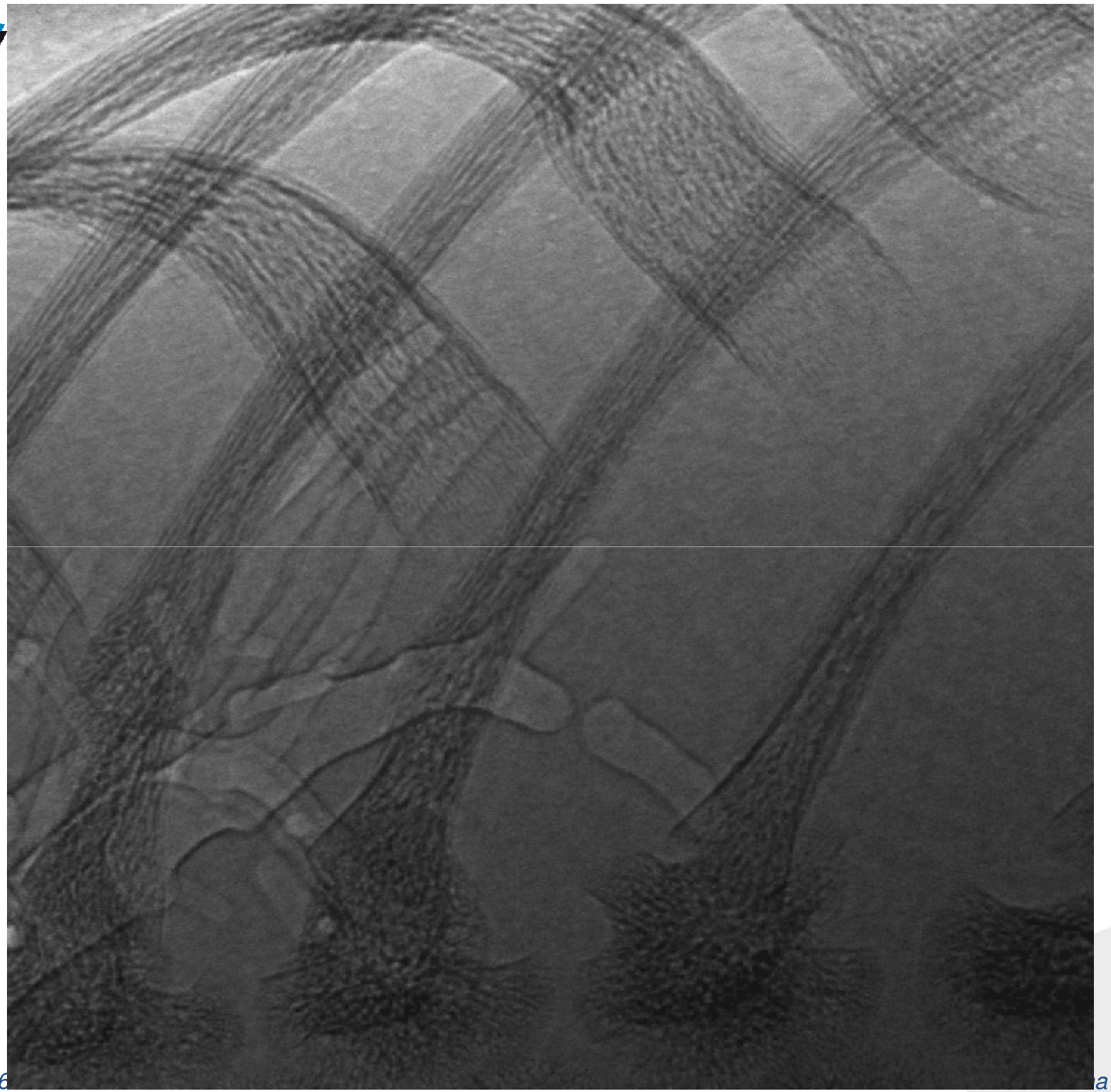

X-ray velocimetry

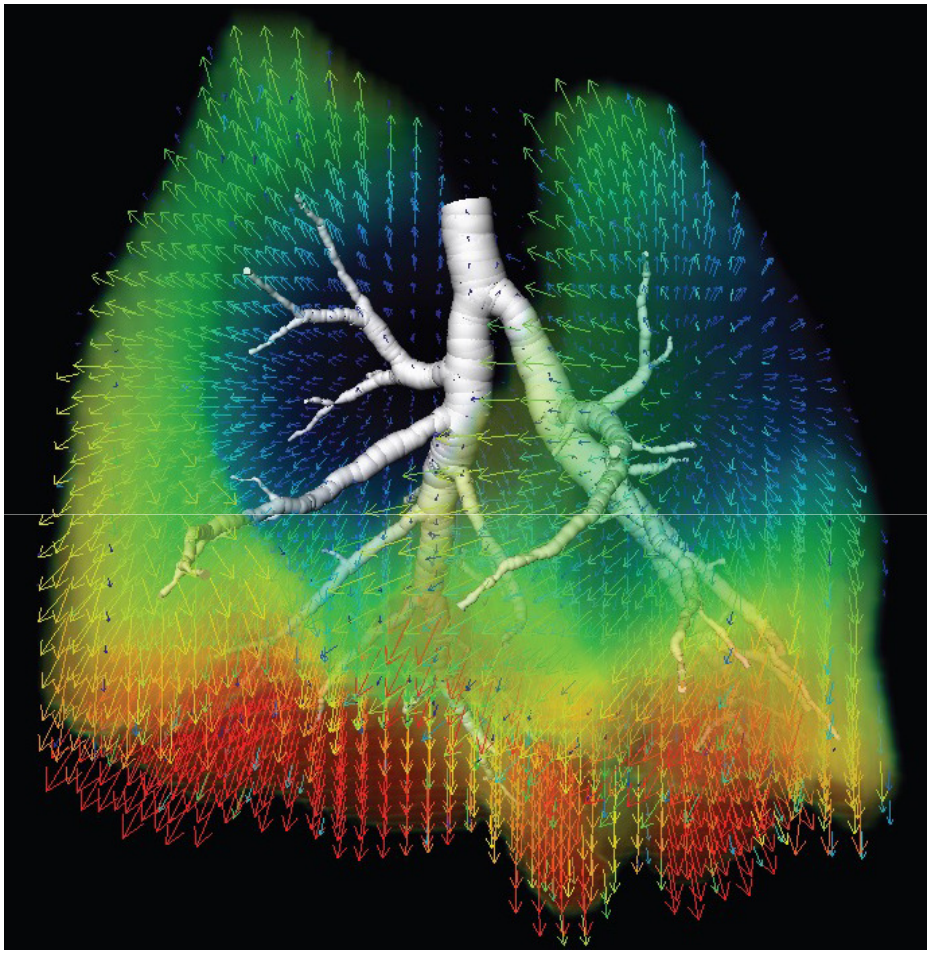

3D map of mouse lung tissue velocity during inspiration. The vectors represent tissue velocity direction, and the colours represent velocity magnitude.
Image courtesy of Steve Dubsky

Brain studies

Technique:	Propagation based Imaging + contrast agent (gold nano particles)
Purpose:	tracking tumor development
Modality:	micro-CT *ex-vivo* imaging on mice
	(recent development: first *in-vivo* experiment)
Technique:	Grating Interferometry
Purpose:	animal model of Alzheimer disease
Modality:	micro-CT *in vitro* imaging of mice brains

Cell tracking studies for imaging brain tumors in rats

Glioblastoma multiforme (GBM) is the most common and aggressive primary brain tumor in humans.
An animal model based on Wistar rats have been developed.

Aim of the cell tracking technique:
monitor the dynamic of tumour growth
follow the migration of tumour cells
understand the dynamic of metastasis spread

Protocol: Glioma cells exposed to colloidal Gold Nano Particles (GNP) were implanted into the brain of adult male Wistar rats under general anesthesia. The animals were allowed to recover and were sacrificed two weeks later.

E.Schultke et al., Eur. J. Radiol.,Vol. 68, 2008

Elettra Sincrotrone Trieste

E = 24 keV
PHC dist. = 80 cm
Num. projections = 720
Ccd pixel size = 14μm

3D rendering of a 4 mm thick volume.

A1 and A2:
Tumor without colloidal gold

B1 and B2:
Tumor developed after implantation of 300,000 gold-loaded cells

In the skull segments (A2 and B2), the hole created for cell implantation is well visible (diameter 0.6 mm).

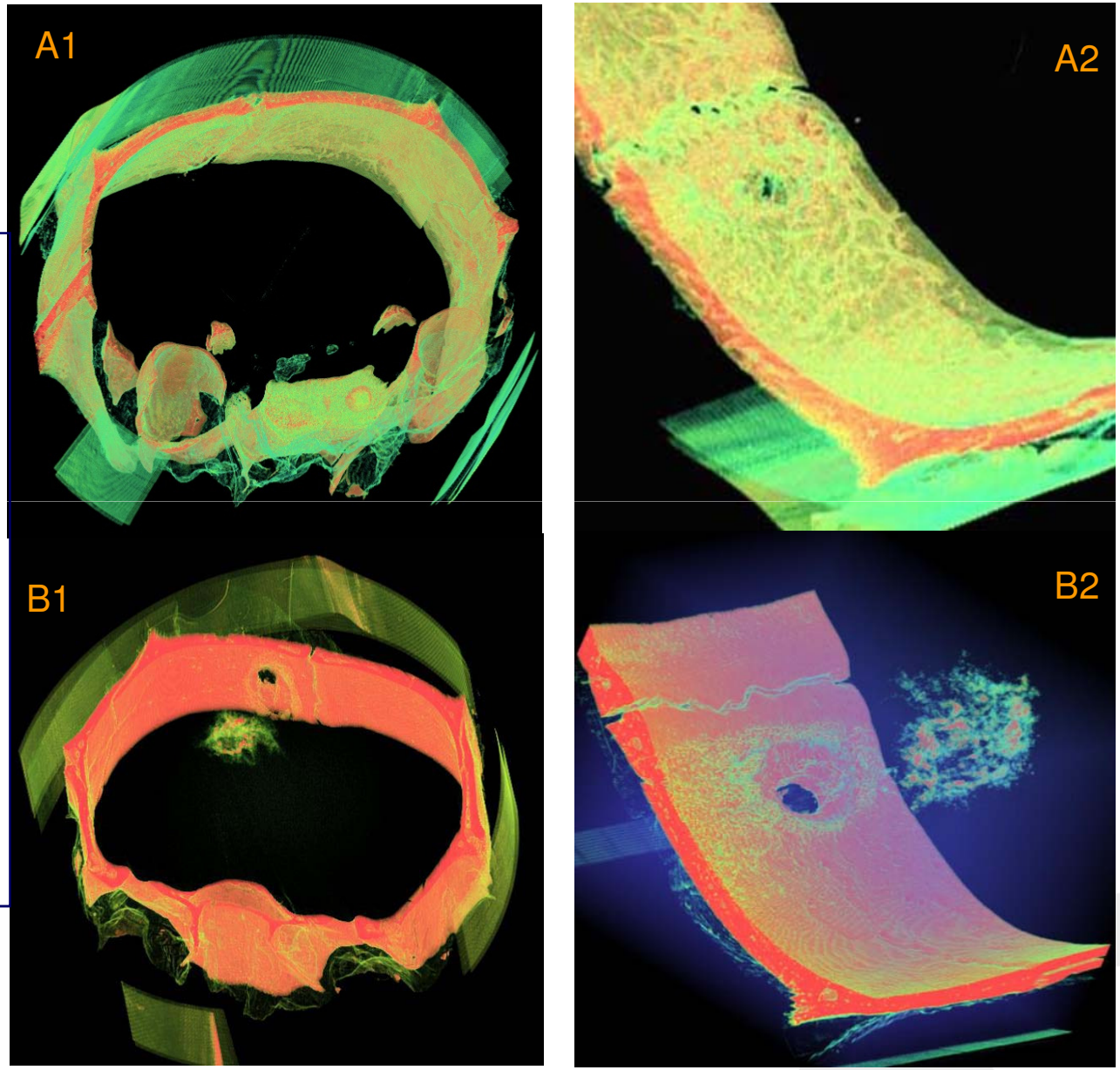

E.Schultke et al., Eur. J. Radiol.,Vol. 68, 2008

Metastasis spread in the spine

Loaded C6 cell are clearly visible in in the periphery of the chord. There is indication that the lesions penetrate into the vertebral bone.

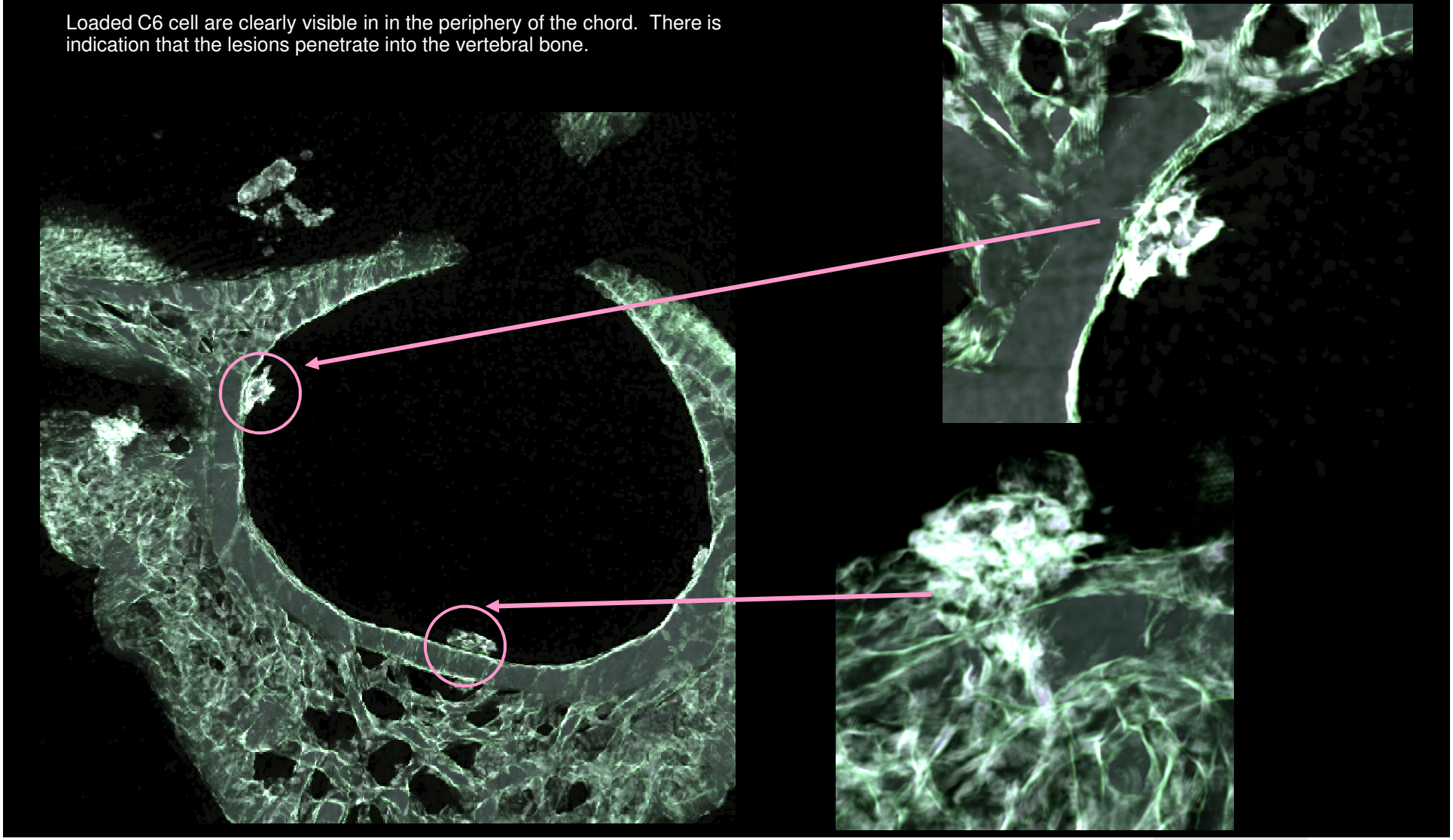

Thick slice obtained with SR

Elettra Sincrotrone Trieste

FIRST In-vivo low dose µ-CT of brain tumors

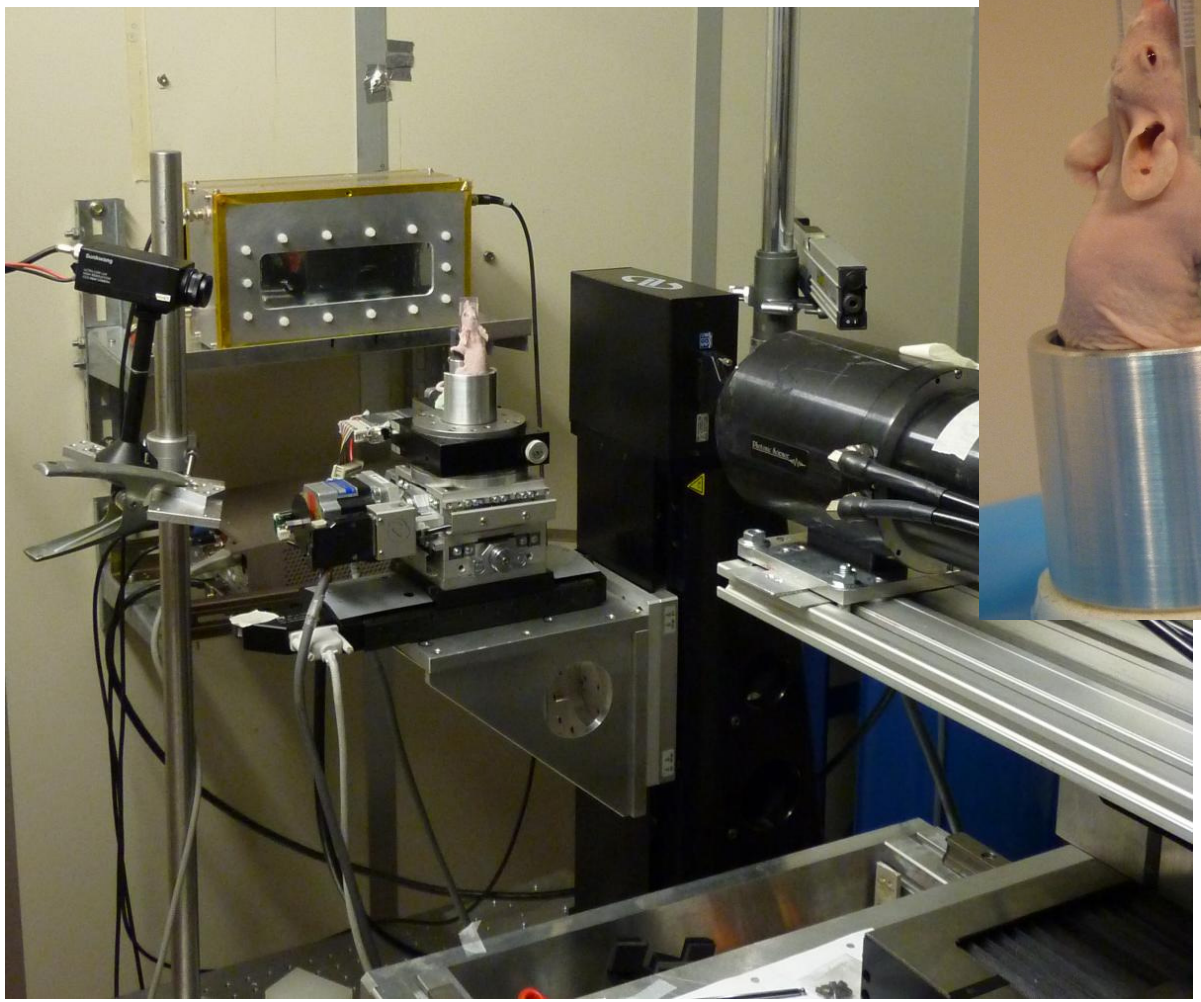

First experiment *in vivo*

A. Astolfo et al., Nanomedicine: Nanotech., Biology and Medicine, Vol. 9, Issue,2013

Elettra Sincrotrone Trieste

Low dose High dose

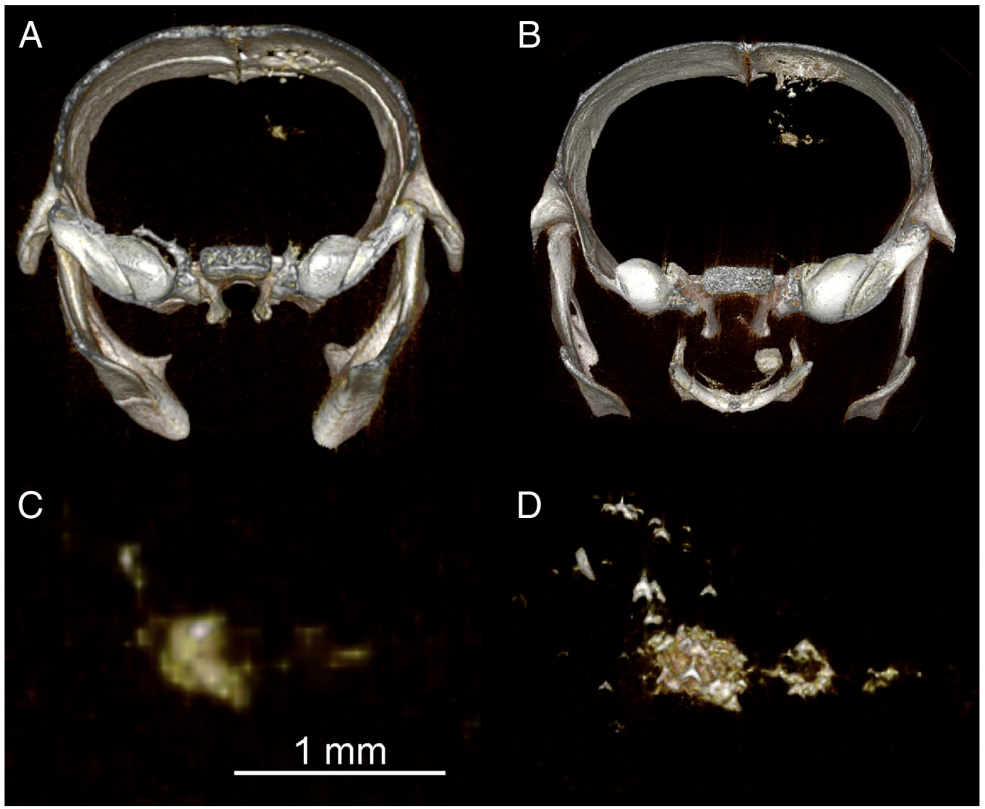

Comparison of two 3D renderings of a CT of a mouse injected with 100,000 GNP-loaded F98 cells depicts (A–C) the low x-ray dose in vivo data and (B–D) the high x-ray dose ex vivo data. The images in panels C and D are enlargements at full system resolution of the developed tumor depicted in panels A and B, respectively.

A. Astolfo et al., Nanomedicine: Nanotech., Biology and Medicine, Vol. 9, Issue,2013

Elettra Sincrotrone Trieste

Studies on Alzheimer's disease

- One of the core pathological features of Alzheimer's disease (AD) is the **accumulation of amyloid plaques** in the brain. Current efforts of medical imaging research aim at visualizing amyloid plaques in living patients to evaluate the progression of the pathology, but also to facilitate the diagnosis of AD.
- Grating Interferometry (GI) has the capability to image amyloid plaques in the brain of a transgenic mouse model of AD. The method provides high contrast and high resolution images. Quantitative analysis can also be performed.
- GI may facilitate the development of other imaging methods such as positron emission tomography (PET) by providing convenient high-resolution 3D data of the plaque distribution for multimodal comparison.
- The study was conducted on a model of AD mouse

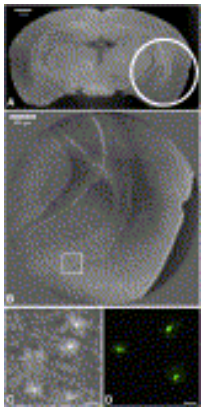

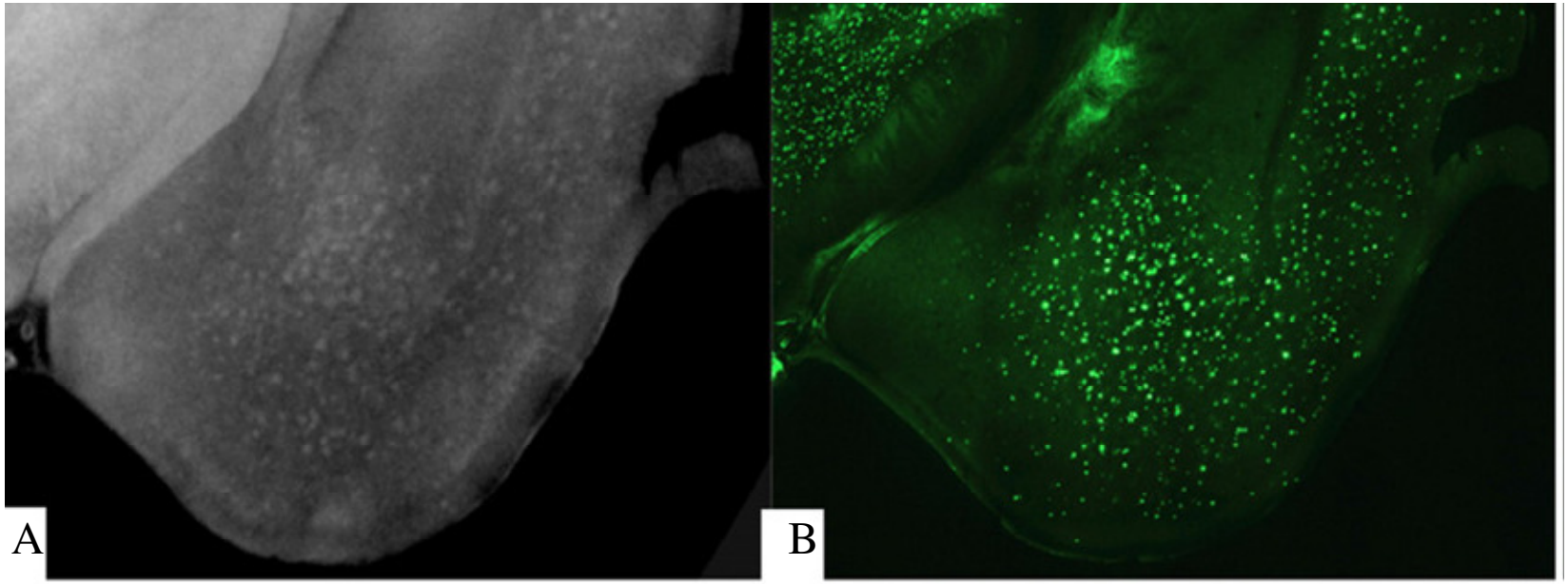

(A) - Magnified unfiltered GI tomograms of a AD transgenic mouse brain at 13 months. The brain was extracted, fixed in paraformaldehyde and scanned by GI based tomography (isotropic voxel size of 7.4 μm). **(B)** - The brain was next sliced at 400 μm and stained with Thioflavin S to reveal amyloid deposits

Pinzer et al ., Neuroimage ***61*** *1336–46, 2012*

Elettra Sincrotrone Trieste

Atherosclerotic plaque imaging

Technique: Propagation- based + staining

Modality: micro-CT *in-vitro* imaging of mice aortas

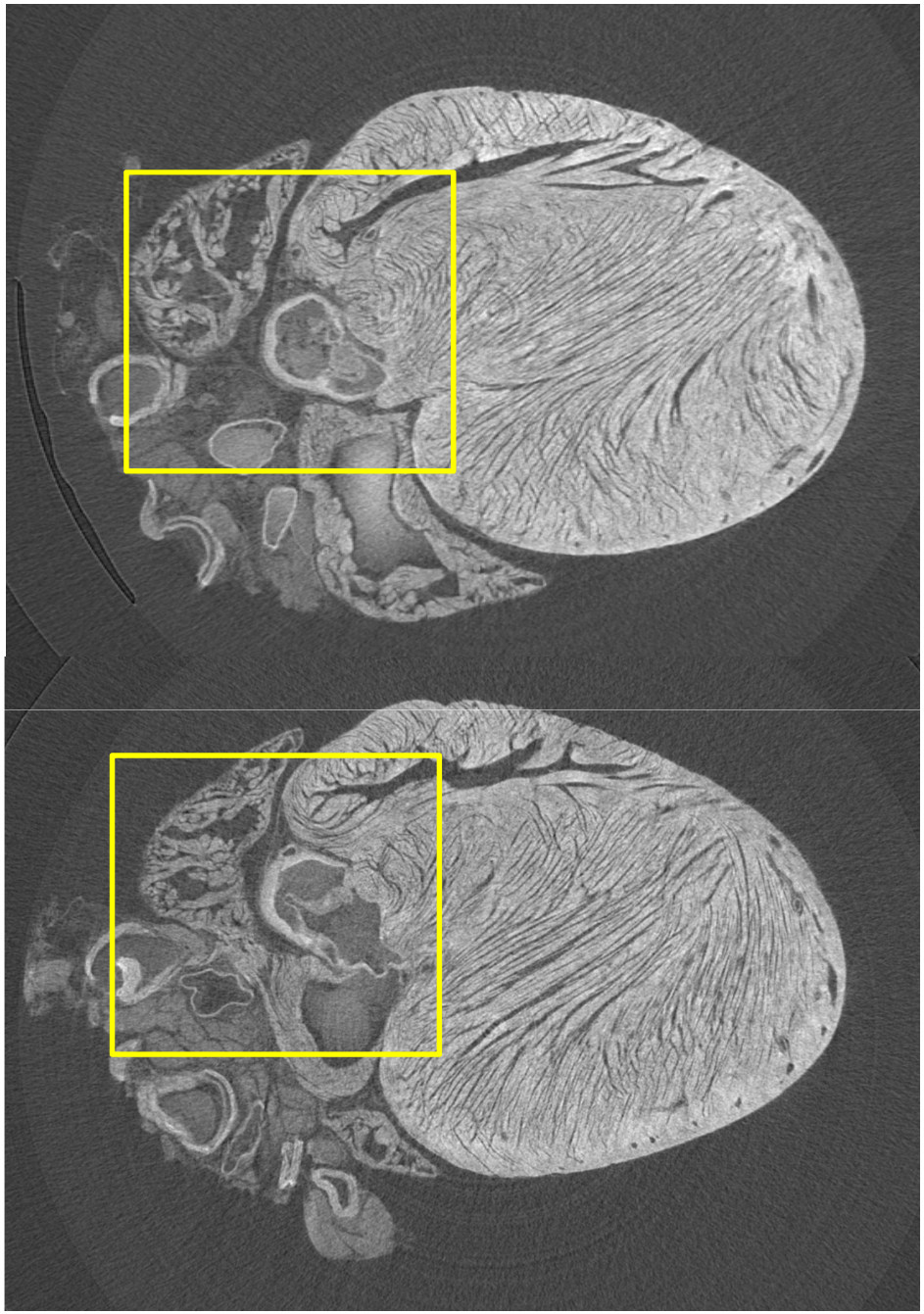

Imaging of atherosclerotic plaques

Animal model: atherosclerotic mouse
Apolipoprotein E-deficient (apoE–/–) mouse

Deficient transgenic mice demonstrates a strong tendency to develop hyper-cholesterolemia

Aim: evaluate the capability of µ–CT to highlight the formation of atherosclerotic plaques in normal and Apo mice
All mice were fed with a high fat diet for 70 days
Imaging procedures:
E = 27 keV, PHC dist = 30 cm
Staining procedure based on PTA (Phosphotungstic acid)

UNIVERSITÄTSMEDIZIN GÖTTINGEN UMG

Elettra Sincrotrone Trieste

Comparing CT slice with histology

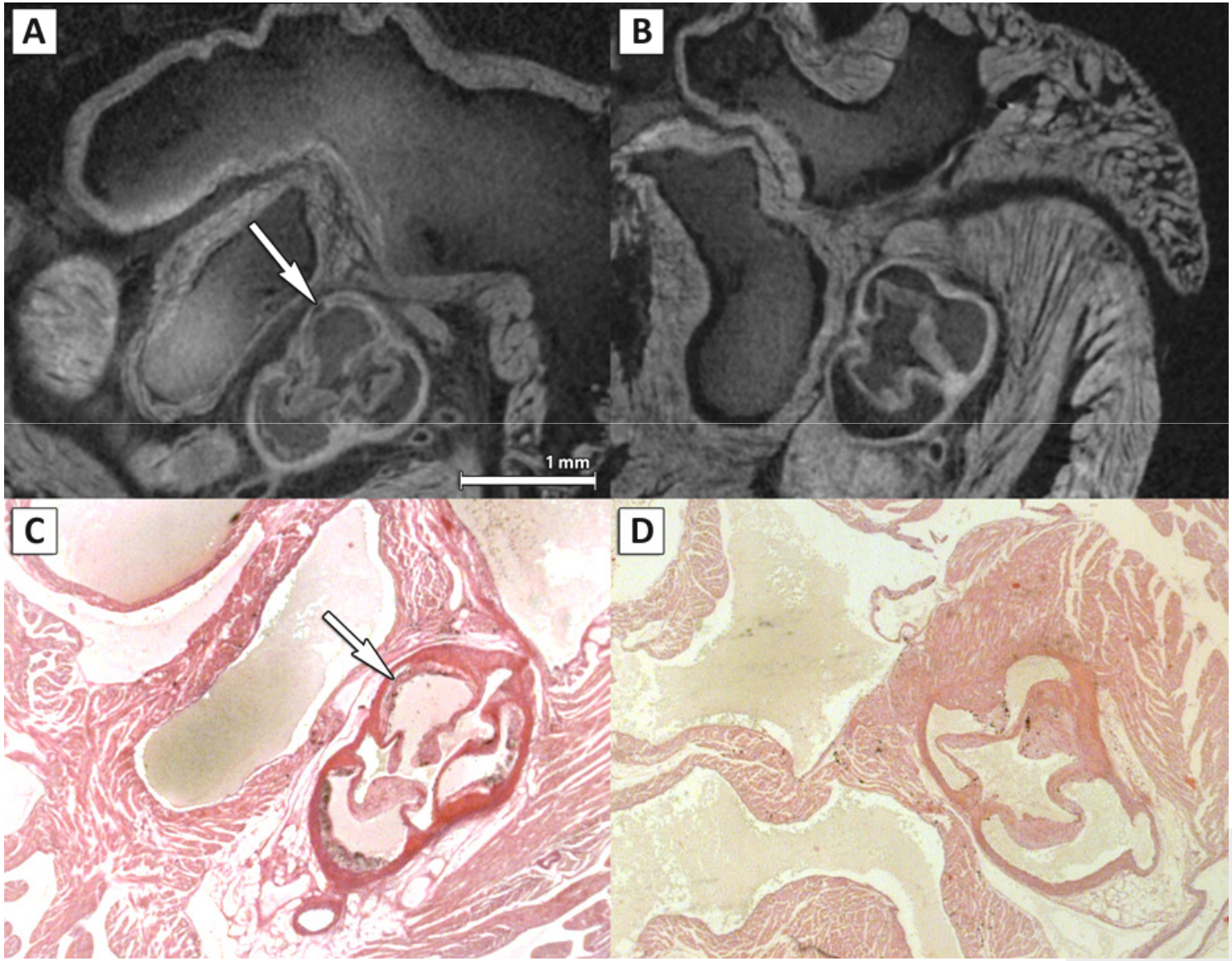

Elettra Sincrotrone Trieste

Micro-CT aplications: quantitative analysis

- Pore3D: A software package developed by the SYRMEP team for analysis of CT reconstructed data
- Some applications

Elettra Sincrotrone Trieste

http://ulisse.elettra.trieste.it/uos/pore3d

Pore3D: a software tool for **3D image processing** & **analysis**

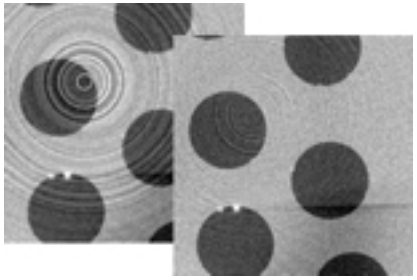

Filters
Basic (mean, median, gaussian, ...)
Anisotropic diffusion
Bilateral
Ring artifacts reduction
Binary (median, clear border, ...)

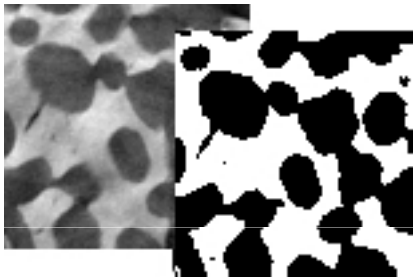

Segmentation
Automatic thresholding (Otsu, Kittler, ...)
Adaptive thresholding
Region growing
Multiphase thresholding
Clustering (*k*-means, *k*-medians, ...)

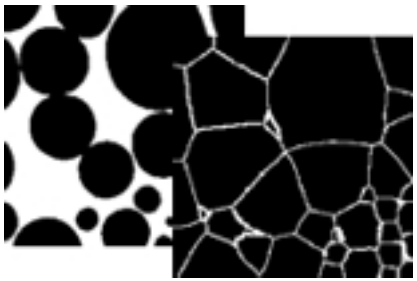

Morphological processing
Dilation and erosion
Morphological reconstruction
Watershed segmentation
Distance transform
H-Minima filter

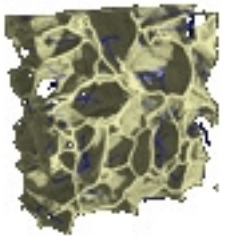

Skeleton extraction
Thinning
Medial axis (LKC)
DOHT
Gradient Vector Flow
Skeleton pruning
Skeleton labeling

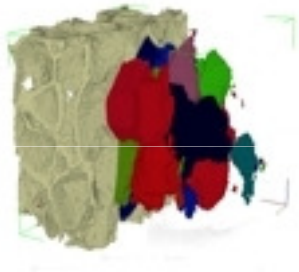

Analysis
Minkowski functionals
Morphometric analysis
Anisotropy analysis
Blob analysis
Skeleton analysis
Textural analysis (fractal dimension, ...)

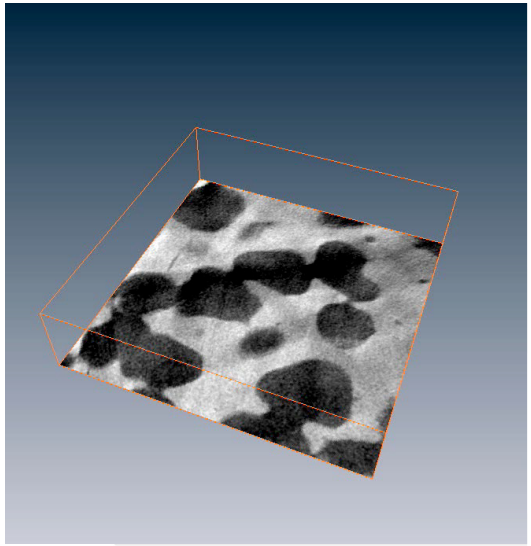

Thanks to the support of the Scientific Computing group, now the software is available also as a SaS (Software as Service) facility for external users.

Francesco Brun et al., NIM A, 615 (2010) 326–332

Bone turnover in mice exposed to micro-gravity conditions

- 3 wild type (WT) mice and 3 pleiotrophin-transgenic (PTN-Tg) mice in a special payload (MDS - Mice Drawer System). The transgenic mouse strain over-expressing pleiotrophin (PTN) in bone was selected because of the PTN positive effects on bone turnover.
- **91 days in the International Space Station (ISS) by NASA: Aug. - Nov. 2009.**
- Controls:
  - mice on Earth in the same special payload MDS (*ground* mice)
  - mice in common cages (*vivarium* mice)
- SR μ-CT experiments were performed on femurs and spines
- Being non-destructive, μ-CT is very attractive for these rare specimens

University of Genova

Università Politecnica delle Marche

University of Trieste – Dept. of Engineering

Analysis of the microarchitecture of the trabecular bone in femurs

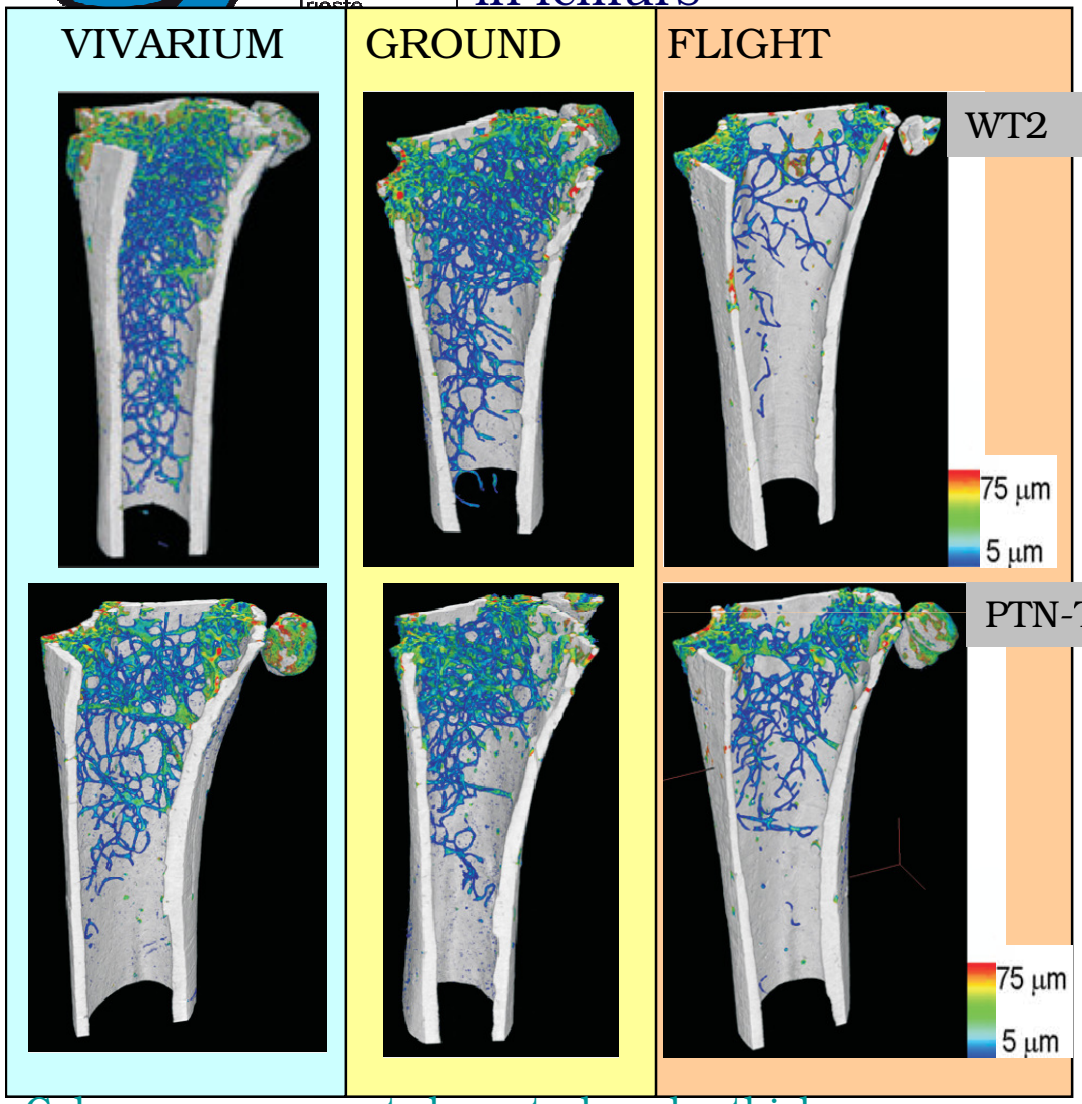

Color map represents bone trabecular thickness distribution in the femur (red = 75 µm, blue = 5 µm)

Revealed:

-a **bone loss** during spaceflight in the weight-bearing bones

-a **decrease** of the trabecular number

-an **increased** mean trabecular separation

-no significant change in trabecular thickness.

-No effects on not weight-bearing bones.

E = 19 keV
Pixel size = 9 mm
N. Proj = 900
Distance sample-ccd= 3 cm

Comparison WT vs.PTN-Tg2:

- PTN-Tg exposed to normal gravity has a poorer trabecular organization than WT mice

- the expression of the PTN gene during the flight resulted in some protection against microgravity's negative effects.

S. Tavella et al "*Bone Turnover in Wild Type and Pleiotrophin-Transgenic Mice Housed for Three Months in the International Space Station (ISS)*", PlosONE, March 2012.

Characterization of urinary stones

Aim: determination of texture, microstructure and mineralogical composition of kidney stones.

Mineralized tissues and bio-mineral structures i.e. bones, teeth, kidney stones are considered as "archives" related to living habits, nutrition and exposure to changing environmental conditions.

Identification of calculi components is useful to evaluate the chance of their new development as well as to choose the terapeutic approach

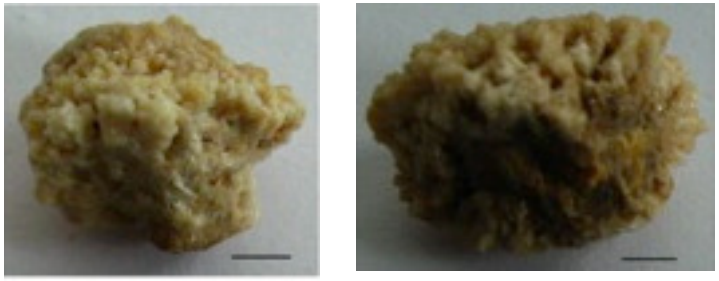

Analyzed urinary calculi fragments no.: 11847 and 11684. The bars have a length of 2 mm.

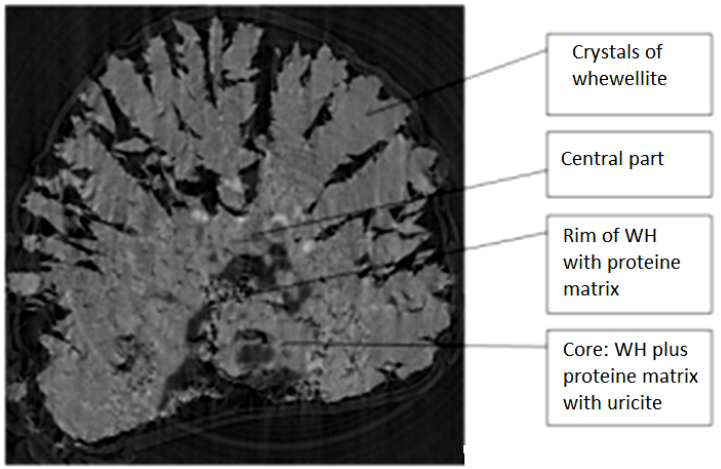

E = 30 keV
Pixel size = 9 mm
N. Proj = 900
Dist. sample-ccd = 50 cm

Texture of urinary calculi - slice n.50 of the sample 11684 situated near the core.

Courtesy of J.Kaiser, M.Hola

Analysis of human kidney stones

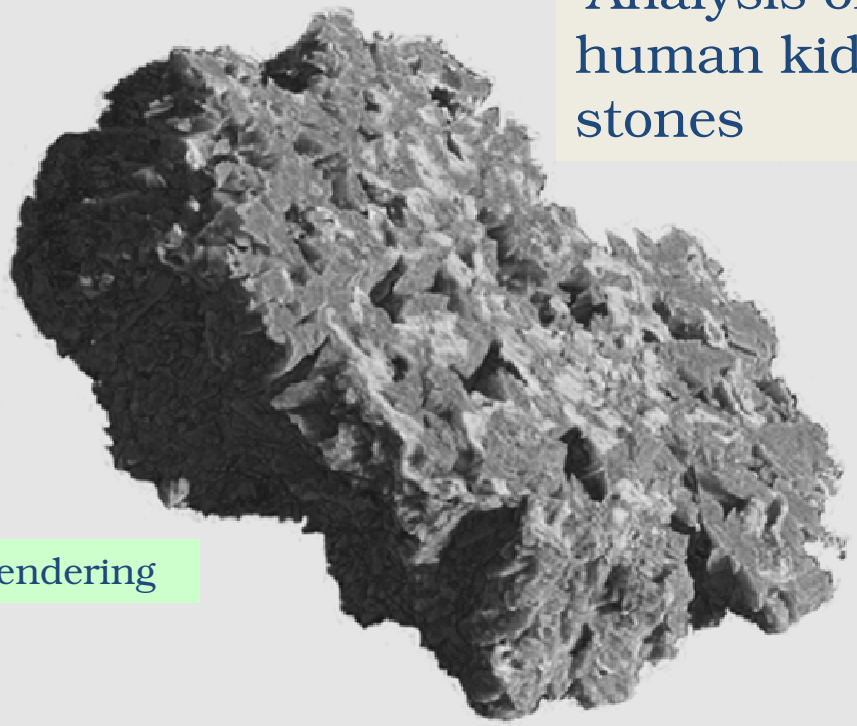

3D rendering

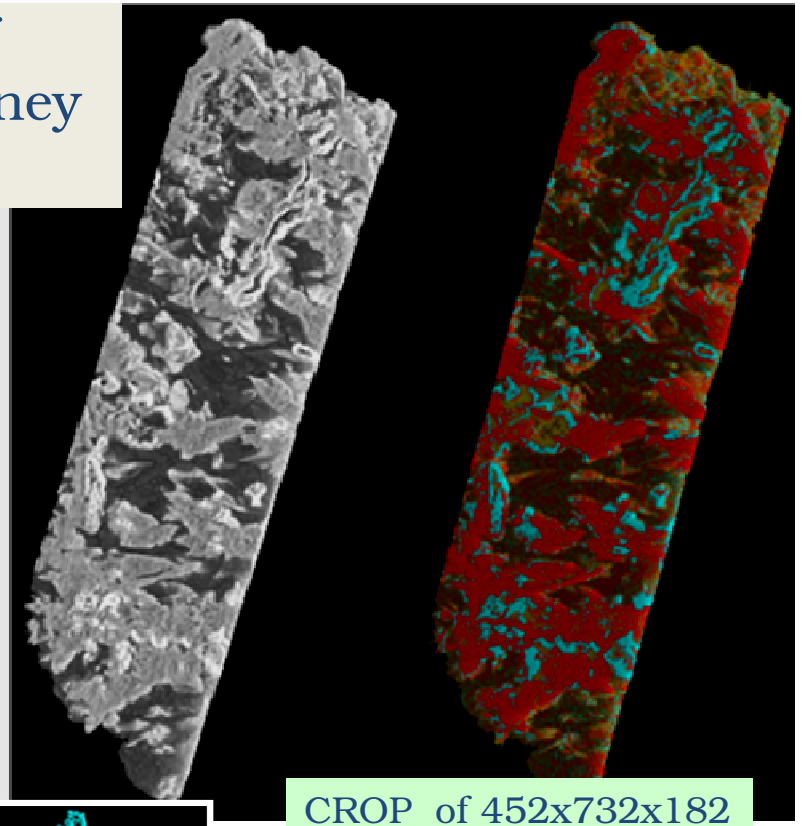

CROP of 452x732x182 pixels of the sample

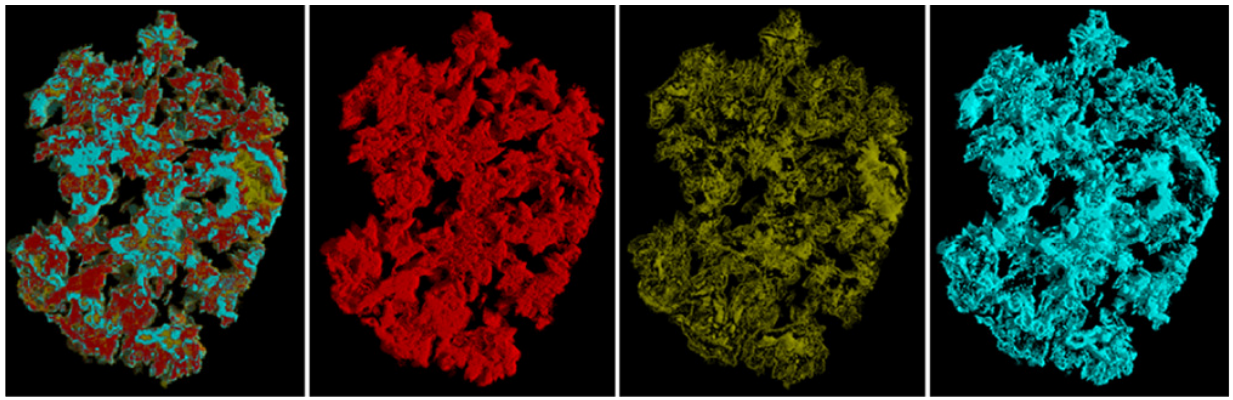

3D rendering of a stack of 20 slices showing the 3 phases segmentation whewellite (red), weddellite (yellow) and apatite (blue)

Volumes (after normalization, taking into account the air pores): are 50.5 % v_{we}/v of **weddelite**, 15.9 % v_{whe}/v of **whewellite**, 33.6% v_{ap}/v of Ca-phosphate „**apatite**“.

J. Kaiser et al., Urological Research, 39 (2011) 259-267.

Elettra
Sincrotrone
Trieste

Contact:
giuliana.tromba@elettra.eu

Thank you for your attention

Talbot interferometry is based on the Talbot effect (1836), which is known as a self-imaging effect observed downstream a grating (object with a periodic structure), under coherent illumination.

The distances z_T between the object and self-imaging planes are determined by the light wavelength λand the period d of the structure

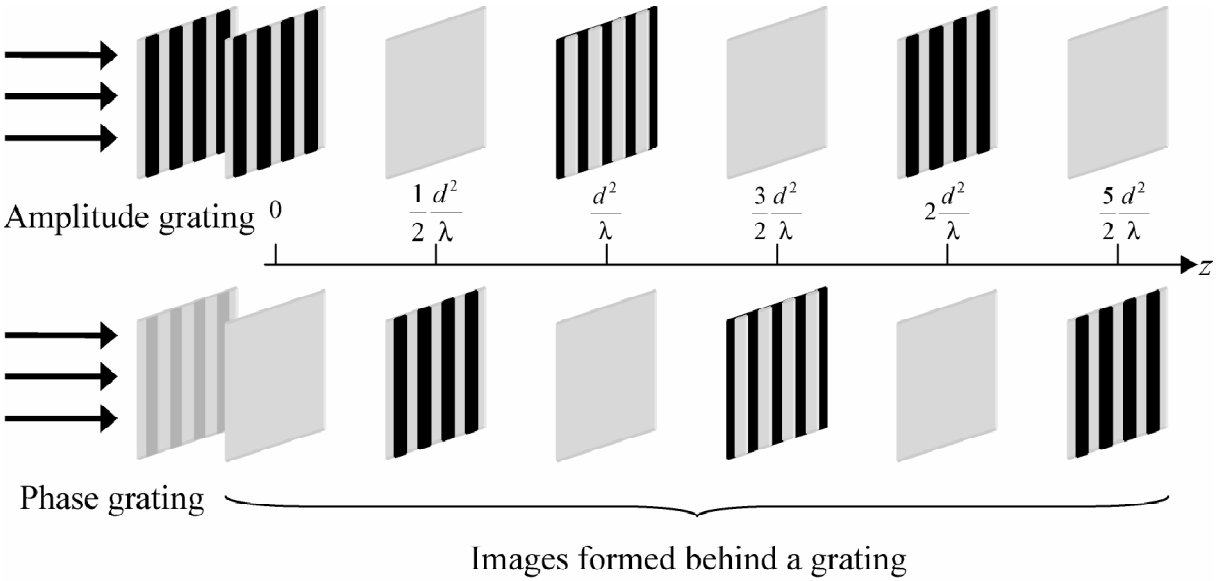

Talbot effect in the case of plane-wave illumination. For **an amplitude grating**, self-images are generated at $z_T = 0, d^2/\lambda, 2d^2/\lambda$, and so on. ($d$ is the period of the grating, λ is the wavelength). For a **phase grating**, similar patterns are observed at intermediate positions.